ACS Sustainable Chemistry & Engineering

Research Article

pubs.acs.org/journal/ascecg

Synergies between Geological Sequestration and Microalgae Biofixation for Greenhouse Gas Abatement: Life Cycle Design of Carbon Capture, Utilization, and Storage Supply Chains

Dajun Yue, Jian Gong, and Fengqi You*

Department of Chemical and Biological Engineering, Northwestern University, Evanston, Illinois 60208, United States

ABSTRACT: We address the integration of two greenhouse gas (GHG) abatement options, namely, geological sequestration and microalgae biofixation, using a supply chain optimization approach. A multiscale, multiperiod, mixed-integer nonlinear programming (MINLP) model is proposed, which accounts for CO_2 transportation pipeline network design, algae processing route, and product selection, as well as the seasonality in CO_2 source availability and algal biomass productivity. The model allows for pipeline transportation of both supercritical CO_2 and feed gas. By using the Life Cycle Optimization framework, we simultaneously optimize the economic and environmental performances. We employ an improved branch-and-refine algorithm for efficient global optimization of the resulting nonconvex MINLP problems. We consider a case study on the optimal design of potential CO_2 capture, utilization, and storage infrastructures in the state of Texas. By taking advantage of the synergies between these two GHG abatement options, the CO_2 emissions can be sequestrated and utilized at an average cost of \$45.52/tCO_2, and about 64% of the GHGs can be avoided from entering the atmosphere.

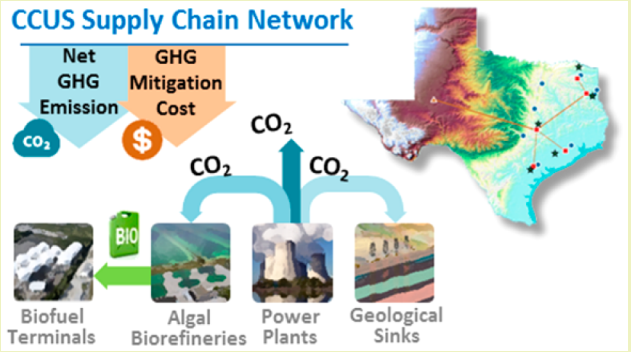

KEYWORDS: *Carbon capture, Utilization and storage, Supply chain design, Life cycle optimization, Geological sequestration, Microalgae biofixation, Multiscale modeling, Branch-and-refine algorithm*

INTRODUCTION

As the primary anthropogenic greenhouse gas (GHG), carbon dioxide (CO_2) is considered to be the leading culprit in global warming and climate change.[1−3] Electric power plants contribute almost 40% of the total CO_2 emissions in the United States, of which about 80% come from the combustion of coal.[4] Under the Clean Air Act,[5] the U.S. Environmental Protection Agency (EPA) has been proposing related plans and standards that aim to considerably cut CO_2 emissions, protect human health, and promote environmental sustainability, especially from the power sector.[6] Considering the large amount of CO_2 to be reduced, carbon capture and storage (CCS) through geological sequestration has been regarded as a major means of GHG abatement.[7−9] Over recent decades, researchers have been working together to answer various questions on technological feasibility and economic efficiency.[10−13] It is not until recently that carbon utilization (CU) through microalgae biofixation was proposed as a new alternative for GHG abatement.[14,15] This option would allow the utilization of CO_2 emitted from large point sources (e.g., a coal-fired power plant) to produce renewable liquid fuels (e.g., diesel) that can be used to displace their fossil fuel-derived counterparts.[16,17] In this work, we investigate how geological sequestration and microalgae biofixation options can be integrated and synergized to form a complete carbon capture, utilization, and storage (CCUS) infrastructure. From the perspective of supply chain optimization, we employ rigorous mathematical programming tools to investigate the underlying economic and environmental potentials.

Two bodies of literature are closely related to the subject of this work. The first body of literature includes works on pipeline network design in CCS projects. These works aim to link the CO_2 point sources with point sinks in an economically efficient manner. Early works on this topic tended to apply simple source−sink matching approaches largely due to the limitations in computing capacity at that time.[18−20] A major drawback of this method is that merging and splitting of CO_2 flows is not allowed, and all captured CO_2 must be transported from one source to one sink in a single pipeline directly. As the total amount of captured CO_2 grows and the numbers of sources and sinks increase, source−sink matching approaches become less capable. Consequently, superstructure-based mathematical programming methods became more popular and are prevalently employed nowadays.[21−24] This approach allows us to capture more important features and develop more sophisticated models. Most existing models are formulated as mixed-integer linear programs (MILP) that account for pipeline routing and pipeline sizing, as well as merging and splitting of

Received: December 19, 2014
Revised: March 10, 2015
Published: April 7, 2015

DOI: 10.1021/sc5008253
ACS Sustainable Chem. Eng. 2015, 3, 841−861

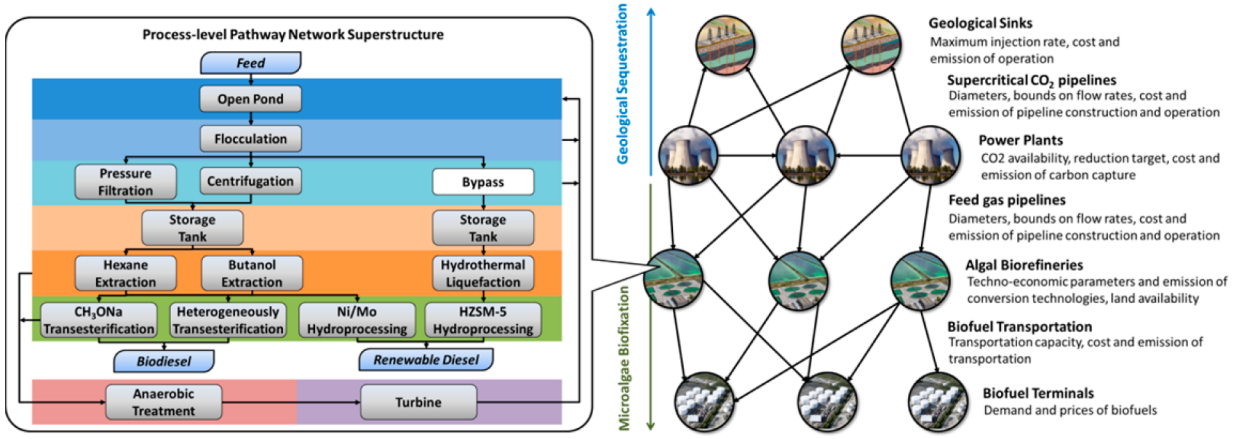

Figure 1. Superstructure of the multiscale CCUS supply chain.

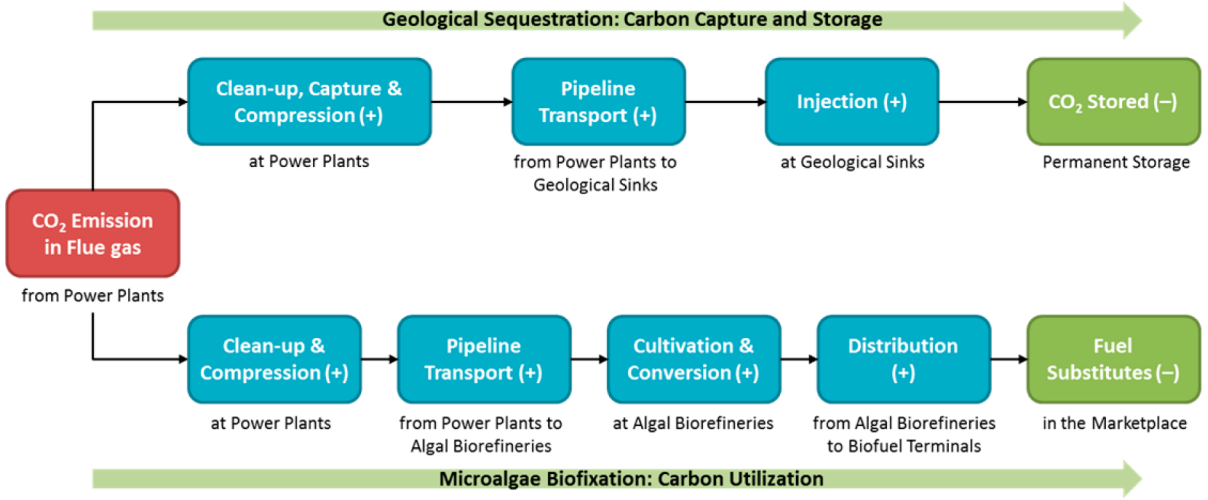

Figure 2. Life cycle stages of the CCUS supply chain.

CO_2 flows. Recently, a mixed-integer nonlinear programming (MINLP) model was proposed to investigate the addition of intermediate pump stations and the impact of pressure drop along pipelines.[25] The second body of literature includes life cycle design works on algae cultivation and processing facilities at algal biorefineries. These works utilize optimization tools to investigate all possible routes for producing algae-based renewable fuels and associated biochemicals.[26−28] Superstructure-based MINLP models were developed to capture the economies of scale while considering mass balance and energy integration constraints.[29,30] By combining this superstructure-based approach with the Life Cycle Optimization (LCO) framework, one could simultaneously optimize the economic and environmental performances of the algal biorefineries.

All of the literature reviewed above investigated geological sequestration and microalgae biofixation as separate options for GHG abatement. However, these two options have the potential to synergistically complement each other. Therefore, we propose a novel superstructure-based MINLP model for an integrated CCUS supply chain. As shown in Figure 1, in a CCS supply chain, the CO_2 emitted from power plants is captured on-site and then transported to geological sinks for permanent storage. On the other hand, in a CU supply chain, the CO_2 as a component of the power plant flue gas is preprocessed and transported to algal biorefineries to serve as primary nutrition for algae cultivation.[31] Through photosynthesis, CO_2 would be converted into organic contents in algal biomass. The lipids can then be extracted and upgraded into biofuels to serve as fossil fuel substitutes in the marketplace.[32] To summarize, the major novelties of this work and the new features of the proposed model are listed below.

- Investigation on the integration of CCS and CU supply chains
- Multiscale modeling and optimization that integrates the scale of supply chain network design and the scale of process design and operations for algal biorefineries
- Multiperiod modeling that captures the seasonality in CO_2 emissions at power plants due to changes in power demand and in lipid productivity at algal biorefineries due to changes in solar irradiation and length of daytime
- Real-world case study in the state of Texas that reveals the economic and environmental potentials of integrating the two GHG abatement options

The rest of this article is organized as follows. We will provide brief introductions on the two GHG abatement options as well as the LCO methodology in the next few sections. The problem under study will be formally stated next, followed by the mathematical model formulation. Tailored global optimization strategies to facilitate the solution process are then

DOI: 10.1021/sc5008253
ACS Sustainable Chem. Eng. 2015, 3, 841−861

presented. We demonstrate the application of this work via a state-level case study with detailed discussions on the results and implications. Conclusions are drawn at the end of the article.

BACKGROUND

Figure 2 summarizes the critical components involved in a CCUS supply chain. The top route is the geological sequestration option for GHG abatement, corresponding to the CCS supply chain, and the bottom route is the microalgae biofixation option for GHG abatement, corresponding to the CU supply chain. In the following sections, we provide an overview of the geological sequestration option, microalgae biofixation option, and LCO framework.

Geological Sequestration. CCS is a technology that can reduce up to 90% of the CO_2 emitted from large point sources.[33−35] The goal is to prevent large quantities of CO_2 from entering the atmosphere.[36,37] As the top route in Figure 2 shows, the CCS supply chain consists of three major stages. In the first stage, CO_2 is separated from the flue gas produced from electricity generation and then compressed for pipeline transportation. The separation of CO_2 includes the removal of particulates, sulfur- and nitrogen-containing compounds (SO_2 and NO_x), dehydration, and carbon capture. Capture technologies can be broadly categorized into three types: postcombustion, precombustion, and oxyfuel combustion.[38] In this work, we consider CO_2 capture with monoethanolamine (MEA), which is one of the most mature postcombustion chemical absorption technologies.[39] The captured CO_2 in the purified streams contributes more than 90 vol % of the gas mixture.[37] After capture, the CO_2 is then compressed and transported to suitable storage sites. As the storage sites are usually far away from the point sources, this is mostly done by pipeline, which is the cheapest way for transporting large quantities of chemically stable fluids for long distances. We note that there are a number of pipeline networks that exist or are under construction in the United States.[40,41] Millions of tons of CO_2 have already been transported annually for commercial purposes. For instance, the United States has been transporting CO_2 by pipeline for enhanced oil recovery projects for four decades.[42] Because gaseous CO_2 has a relatively lower density and mass flow rate, CO_2 is usually transported as a supercritical fluid in pipelines to guarantee an efficient mass flow rate. This requires compression of CO_2 at the power plants and keeping the pressure above a certain threshold (e.g., 8.6 MPa) to avoid vaporization.[25] Therefore, the selected pipeline size must match the corresponding CO_2 mass flow rate. There is another advantage of transporting CO_2 as supercritical fluid; supercritical CO_2 provides a high-pressure driving force that facilitates injection at storage sites. Various underground geological formations can be used as storage sites, including oil fields, gas fields, saline formations, unmineable coal seams, and saline-filled basalt formations.[39] It is believed that well-selected, designed, and managed geological storage sites are likely to retain over 99% of the injected CO_2 over 1000 years with slim leakage.[43] There have been a number of CCS pilot plants installed and in operation, and several large-scale power plant CCS projects are under construction or planning worldwide.[44] The long-distance transportation of CO_2 is well understood and has excellent health and safety records.[45] Therefore, the commercial deployment of the geological sequestration option for GHG abatement can be readily implemented given the support of government incentives and policies.

Microalgae Biofixation. Biofixation of CO_2 by microalgae is a technology that is based on the use of solar energy through photosynthesis to capture and utilize CO_2 streams produced from power plants.[16] As in the case of other biomass options, GHG abatement can be achieved by the conversion of the harvested algal biomass into renewable biofuels that can be used as a substitute for fossil fuels in the marketplace. As the bottom route in Figure 2 shows, the CU supply chain consists of four major stages. In the first stage, flue gas from electricity generation is preprocessed to remove particulates, sulfur- and nitrogen-containing compounds (SO_2 and NO_x), and water. We call the purified flue gas after contaminant removal feed gas, as it will be used as the feed stream for algae cultivation facilities. The feed gas typically contains 15 vol % CO_2 with the balance being nitrogen gas. The feed gas is transported to algal biorefineries, mostly by pipeline. It is worth noting that CO_2 is not separated at the power plants but is instead transported as compressed gas along the pipelines. This approach is due to two reasons. First, a pure CO_2 stream will suffocate the algae.[46] Second, supercritical CO_2 is not necessary for algae cultivation, and regasification facilities can be costly to build. Through a photosynthesis reaction, algae convert the CO_2 in the feed gas into lipids. In comparison with conventional energy crops, algae require less land use and can be deployed on nonarable lands. In addition, algae can accumulate up to 80% lipids in its dry cell weight, significantly increasing the energy density of algal biomass. However, a bottleneck of microalgae biofixation is that algae require more water in cultivation and conversion processes compared to other biomass feedstocks.[47,48] Thus, water constraints must be considered when locating algal biorefineries.[49] A number of technologies are available that convert the lipid contents in algal biomass into renewable biofuels.[50] We consider some relatively mature technologies in this work. As shown in Figure 1, we explicitly model multiple processing sections in algal biorefineries rather than a single-stage input−output model of the entire algal process. In certain sections, a number of process alternatives are available. Waste streams recycling is also considered to improve resource efficiency. The last segment of the CU supply chain is distribution of algal biofuels to the marketplace as a substitute for their fossil fuel-derived counterparts, thus avoiding CO_2 emissions from the production and use of fossil fuels.

Life Cycle Optimization. To simultaneously optimize the economic and environmental performances of the integrated supply chain, we adopt the established LCO framework, which systematically integrates the life cycle analysis methodology and multiobjective optimization techniques. LCO has been pursued by researchers in a variety of applications.[51−58] As described in ISO standards,[59] a life cycle analysis consists of four phases: goal and scope definition, life cycle inventory analysis, life cycle impact assessment, and life cycle interpretation. The life cycle analysis methodology measures the environmental impact of a given product system.[60] However, it cannot automatically generate alternatives for comparison and identify the optimal one.[61−63] By coupling the last phase of life cycle analysis with multiobjective optimization, the LCO framework is able to reveal the trade-off between economic and environmental performances and produce a series of Pareto-optimal solutions.

The major life cycle stages involved in an integrated CCUS supply chain are summarized in Figure 2. The red block on the left denotes the CO_2 (as a component of flue gas) emitted from

DOI: 10.1021/sc5008253
ACS Sustainable Chem. Eng. 2015, 3, 841−861

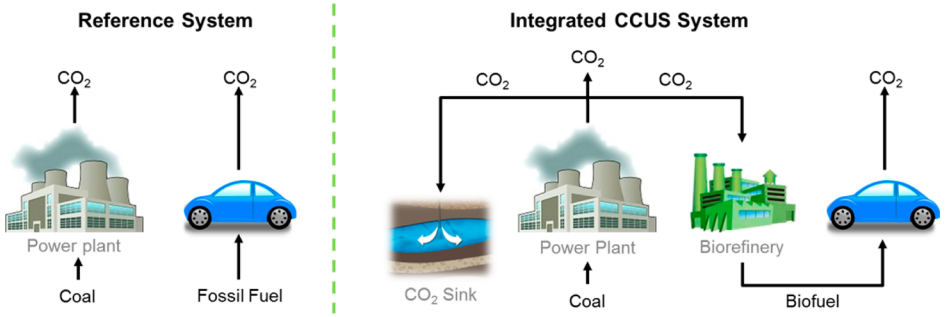

Figure 3. Illustration of the reference system and integrated CCUS system.

the power plants. Two GHG abatement options are considered to deal with the CO_2. Processes that have net positive GHG emissions are denoted with a "+" sign, and those that have net negative GHG emissions are denoted with a "−" sign. In the CCS supply chain, capture and compression of CO_2, transport of supercritical CO_2 through pipelines, and injection of CO_2 into geological formations all result in net positive GHG emissions, while GHG abatement in the geological sequestration option is achieved by permanent storage of the captured CO_2 underground. In the CU supply chain, stages that have net positive GHG emissions include cleanup and compression of feed gas, transportation of feed gas through pipelines, cultivation and conversion of algal biomass, and distribution of the produced renewable biofuels to their respective terminals. Unlike geological sequestration, microalgae biofixation reduces GHG emissions indirectly.[64] By substituting fossil fuels in the marketplace with renewable biofuels, we can avoid the GHG emissions associated with the production, distribution, and combustion phases of those fossil fuels. Note that the power plants with CCUS may have lower net electricity output because the carbon capture and separation processes consume electricity from the power plants. Therefore, the corresponding GHG emissions related to the generation and use of this electricity must be accounted for in the calculation. Given the short span of the time for which the CO_2 is stored in the biofuel products, the release of CO_2 to the atmosphere by the combustion of biofuels must also be accounted for in the calculation.

Global warming potential (GWP) with respect to a 100-year time frame is chosen as the impact assessment model, which specifies an impact factor to every GHG species and aggregates the environmental impacts of all GHGs in the life cycle inventory into a single indicator in terms of CO_2-eqivalent.[65] According to the GWP model in EcoInvent v2.2,[66] we employ the following equation to account for a total of 32 species of GHGs. Some major species and their GWP are CO_2 (1), CH_4 (25), N_2O (298), hydrofluorocarbons (124−14,800), etc.

$$GWP = \sum_{spc} \omega_{spc} \cdot LCI_{spc}$$

where *spc* denotes the index of GHG species. ω_{spc} is the impact factor of species *spc*. LCI_{spc} is the life cycle inventory of species *spc*. Note that all the environmental parameters are given in terms of GWP. Unless otherwise specified, wherever the term "GHG emissions" or "CO_2-eqivalent" is used, it refers to the aggregation of GHGs according to GWP. The term "CO_2" is only used to quantify the flow rate of pure CO_2 in power plant emissions, supercritical CO_2 pipelines, and feed gas pipelines.

Instead of calculating the absolute value of the life cycle GHG emissions, we focus on the relative difference in GHG emissions between the integrated CCUS system and a reference system.[26] This difference is defined as the amount of GHGs avoided in this work. As shown in Figure 3, there is neither CCS nor CU in the reference system. The total amount of CO_2 produced from the power plants are the same for both systems. Note that the upstream stages (e.g., fuel production, supply) related to the coal-fired power plants are also the same for both systems. Therefore, the GHG emissions of these upstream stages do not influence the calculation of the amount of GHGs avoided. Assuming that the biofuels produced in the integrated CCUS system substitute the same amount of conventional liquid transportation fuels, the GHG emissions related to the production and combustion of the conventional liquid transportation fuels in the reference system can be avoided. Different from the functional unit-based LCO approach[67,68] that minimizes the GHG emissions related to per unit of product output (e.g., electricity, fuel), we tend to maximize the amount of GHGs avoided from a fleet of given power plants by building the integrated CCUS system.

PROBLEM STATEMENT

The problem addressed in this work is formally stated as follows and aims to reveal the economic and environmental potentials of integrating the geological sequestration and microalgae biofixation options for GHG abatement.

The superstructure of the integrated CCUS supply chains is shown in Figure 1. All of the facilities are denoted by a set of nodes (indexed by *l*). To facilitate the presentation, we introduce two aliases of index *l*: *lp* and *lpp*. The nodes in the supply chain network include a set of power plants (*Pow*), a set of geological sinks (*Sink*), a set of algal biorefinery candidate sites (*Bio*), and a set of biofuel terminals (*Lcus*). The power plants are sources of CO_2 emissions, where the monthly CO_2 output and corresponding unit capture costs and emissions are given. The geological sinks are permanent storage sites for CO_2, and the storage capacity and corresponding unit sequestration costs and emissions are given. The algal biorefineries convert CO_2 into lipids, which are further upgraded into renewable biofuels on-site. A detailed process design and optimization model is adapted from the work of Gong et al.[50] and embedded into this supply chain superstructure. A number of promising conversion routes are included, which leads to multiscale modeling with significantly higher fidelity. In the last stage, final algal biorefinery products (indexed by *prd*) are shipped to biofuel terminals that serve the customers, where the demand levels and corresponding market prices are given. Emissions related to the final products are counted as credits to the supply

DOI: 10.1021/sc5008253
ACS Sustainable Chem. Eng. 2015, 3, 841−861

chain system. There are three types of arcs that link the four types of nodes. Arcs between power plants and geological sinks are linked by pipelines transporting supercritical CO_2. A set of standard pipeline diameters (indexed by *dia*) are available for choice, each with specified upper and lower bounds on the mass flow rate. Following the assumptions by Middleton and Bielicki[21] and Zhou et al.,[25] we allow for the connection of supercritical CO_2 pipelines between power plants. This adds more freedom to the design of pipeline network and can lead to potentially lower pipeline cost. Arcs between power plants and algal biorefineries are linked by pipelines transporting feed gas. A set of standard pipeline diameters (indexed by *diag*) are available for choice, each with specified upper and lower bounds on the mass flow rate. The arcs between algal biorefineries and biofuel terminals are linked by road transportation, and the costs and emissions of transporting a unit weight over a unit distance are given. The distances of the arcs on Earth can be estimated using great circle distances[69] or obtained with the help of geographic information systems (GIS). A brief summary of parameters in different parts of the integrated CCUS supply chain is given on the right of Figure 1. Observing that the changes in solar irradiation and length of daytime can influence the productivity of algal biomass, we employ multiperiod modeling techniques to capture the seasonality in supply chain operations. In particular, we divide the planning horizon into a set of equal-length time periods (indexed by *t*) and consider two different operating modes (indexed by *mds*), namely, daytime and nighttime. It is assumed that there is no production of algal biomass at night. An option of using artificial sunlight at night is not considered as it is not energy efficient. Annual discount rate and projected lifetime are also given for the calculation of discounted cash flows.

The goal is to minimize the CO_2 reduction cost and at the same time maximize the amount of CO_2 avoided from entering the atmosphere. This is achieved by optimizing the following strategic and operational decisions:

- Pipeline routing and diameter selection for the transport of supercritical CO_2 and gaseous feed gas
- Matching of CO_2 quantities between power plant point sources and geological sinks and consumptions at algal biorefineries in different time periods and operating modes
- Number, locations, sizes, and selected technologies of the algal biorefineries
- Production profiles at the installed algal biorefineries
- Transportation levels of the shipment of biofuels from algal biorefineries to biofuel terminals

MODEL FORMULATION

A multiscale, multiperiod model is developed to address the problem stated above. This model is developed based on a number of previous models. The models by Middleton and Bielicki[21] and Zhou et al.[25] provide a basis for design of CO_2 pipeline networks. The model by Gong and You[50] is adapted for the design of algal biorefineries. The model by You and Wang on biofuel supply chains[70] sheds light on multiperiod planning of biofuel production and logistics. Two objectives are considered as we are interested in both the economic and environmental performances of the integrated CCUS supply chain. Constraints 1−4 are for the power plants. Constraints 5−6 are for the geological sinks. Constraints 7−14 are for the algal biorefineries. Constraints 15−21 are for pipeline transportation of supercritical CO_2 from power plants to geological sinks. Constraints 22−28 are for pipeline transportation of feed gas from power plants to algal biorefineries. Constraint 29 is for biofuel transportation from algal biorefineries to biofuel terminals. Constraints 30−31 are for the biofuel terminals. Constraints 32−39 are for the cost calculations. Constraints 40−46 are for the environmental evaluations. A list of indices, sets, parameters, and variables is given in the Nomenclature section, where all parameters are denoted in lower case symbols or Greek letters, and all variables are denoted with capitalized initials. The model for the design and operations of algal biorefineries is adapted from the work by Gong et al.[50] with minor changes. Therefore, the detailed biorefinery process model is placed in Appendix A to avoid duplication.

Power Plants. CO_2 emissions in the flue gas from power generation can be treated in two ways. In the geological sequestration option, CO_2 is captured and separated from the flue gas. In the microalgae biofixation option, CO_2 is retrieved as feed gas after contaminant removal. The total mass flow rate of the captured CO_2 ($Gcd_{l,t,mds}$) plus the CO_2 retrieved as a component of feed gas ($Ggcd_{l,t,mds}$) cannot exceed its availability ($acd_{l,t}$). To account for the loss of CO_2 during capture or retrieval processes, we consider a loss factor ($\eta_{l,t}$) in the following equation.

$$Gcd_{l,t,mds} + Ggcd_{l,t,mds} \le (1 - \eta_{l,t}) \cdot acd_{l,t}, \quad \forall\, l \in Pow,\ t,\ mds \tag{1}$$

An annual CO_2 emissions reduction target (tgt_l) must be met at each power plant in line with recent EPA legislations and mandates.[6] The following constraint allows the power plants to control the quantity of CO_2 emissions to capture and utilize in each time period and operating mode, as long as the annual reduction target is met.

$$\sum_{t} \sum_{mds} \tau_{t,mds} (Gcd_{l,t,mds} + Ggcd_{l,t,mds}) \ge \sum_{t} tgt_l \cdot acd_{l,t}, \quad \forall\, l \in Pow \tag{2}$$

where $\tau_{t,mds}$ indicates the length of operating mode *mds* in time period *t*.

The supercritical CO_2 mass balance at power plants is modeled by the following equation. We assume that supercritical CO_2 streams can be merged and split at point sources. Therefore, the total mass flow rate of the received CO_2 plus that of the captured CO_2 on-site should balance the total mass flow rate of the outgoing supercritical CO_2.

$$\sum_{lp \in Adj_l} Qcd_{lp,l,t,mds} + Gcd_{l,t,mds} = \sum_{lpp \in Adj_l} Qcd_{l,lpp,t,mds}, \quad \forall\, l \in Pow,\ t,\ mds \tag{3}$$

By definition, $Qcd_{l,lp,t,mds}$ is the mass flow rate of supercritical CO_2 transported from node *l* to node *lp* in time period *t* and operating mode *mds*. Therefore, $Qcd_{lp,l,t,mds}$ denotes flow from node *lp* to node *l*, and $Qcd_{l,lpp,t,mds}$ denotes flow from node *l* to node *lpp*. To eliminate unpromising links, we assume that pipelines for supercritical CO_2 can only be installed between certain adjacent nodes (Adj_l).

The gaseous CO_2 is transported as a component of feed gas to algal biorefineries to serve as nutrition for algae cultivation. The mass balance relationship is expressed as follows.

DOI: 10.1021/sc5008253
ACS Sustainable Chem. Eng. 2015, 3, 841−861

$$Ggcd_{l,t,mds} = \sum_{lp \in Nbr_l} Qgcd_{l,lp,t,mds}, \quad \forall\, l \in Pow,\ t,\ mds \tag{4}$$

where $Qgcd_{l,lp,t,mds}$ is the mass flow rate of gaseous CO_2 transported from node l to node lp in time period t and operating mode mds. To avoid building feed gas pipelines over unrealistically long distances, we assume that feed gas can only be transported to algal biorefineries that are near the power plant (Nbr_l).

Geological Sinks. The mass flow rate of the supercritical CO_2 received at the geological sinks should be equal to the flow rate that is injected ($Scd_{l,t}$) into the underground geological formations. This mass balance relationship is modeled by the following equation.

$$\sum_{lp \in Adj_l} Qcd_{lp,l,t,mds} = Scd_{l,t}, \quad \forall\, l \in \sin k,\ t,\ mds \tag{5}$$

The injection rate cannot exceed the maximum injection rate of the geological sink ($scap_l$).

$$Scd_{l,t,mds} \le scap_l, \quad \forall\, l \in \sin k,\ t,\ mds \tag{6}$$

Algal Biorefineries. The mass flow rate of the gaseous feed gas received at the algal biorefineries should be equal to that consumed in algae cultivation ($Hcd_{l,t,mds}$). The conservation of mass is given below.

$$\sum_{lp \in Nbr_l} Qgcd_{lp,l,t,mds} = Hcd_{l,t,mds}, \quad \forall\, l \in Bio,\ t,\ mds \tag{7}$$

The correlation between the amount of CO_2 consumed and the quantity of renewable biofuels produced is established by the process model in Appendix A regarding the design and operations of algal biorefineries. Here, we will only list a number of interface constraints 8−11 that link the supply chain model with the process model. For clarity, all variables from the process model are marked with the superscript (p).

The following equations indicate that the algae cultivation facility within an algal biorefinery only consumes CO_2 during daytime. Note that although there is no production of algal biomass at night, sections other than cultivation, harvesting, and dewatering are still operating. This is achieved due to the addition of biomass storage in algal biorefineries so that algal biomass can be stored for conversion at night (which is accounted for in the process model).

$$Hcd_{l,t,day} = \omega \cdot Hcd_{l,t}^{hr(p)}, \quad \forall\, l \in Bio,\ t \tag{8}$$

$$Hcd_{l,t,night} = 0, \quad \forall\, l \in Bio,\ t \tag{9}$$

where ω is a factor that converts monthly flow rates to the hourly flow rates used in the process model.

Because biofuels are produced in the upgrading section, the production amount of biofuel products ($Wprd_{l,prd,t}$) is linked to the process variables of "down" flow at the upgrading stage ($Mr_{t,l,i,j,k}^{down(p)}$). This relationship is given below. Note that the subset prd belongs to the set of species k used in the process model.

$$Wprd_{l,prd,t} = \sum_{j} Mr_{t,l,upgrading,j,prd}^{down(p)}, \quad \forall\, l \in Bio,\ prd,\ t \tag{10}$$

The land area available at each algal biorefinery candidate site ($land_l$) can be different. Therefore, the capacity of the algal biorefinery may be limited by the following land use constraint.

$$Area_l^{(p)} \le land_l, \quad \forall\, l \in Bio \tag{11}$$

where $Area_l^{(p)}$ is the process variable that represents the occupied area of algal biorefinery l.

Considering the constraints on government policies and capital investment, we might want to limit the total number of algal biorefineries to build. This is modeled by the following logic constraints.

$$Xb_l \ge Y_{l,i,j}^{(p)}, \quad \forall\, l \in Bio,\ i,\ j \tag{12}$$

$$\sum_{l \in Bio} Xb_l \le nb \tag{13}$$

where Xb_l is a binary variable, which is equal to 1 if algal biorefinery l is built. $Y_{l,i,j}^{(p)}$ is a binary variable belonging to the process model, which is equal to 1 if technology j in section i is chosen at algal biorefinery l. The maximum number of algal biorefineries allowed to build is represented by nb.

The final products produced at the algal biorefineries are shipped to biofuel terminals; from there, they are distributed to customers. This mass balance relationship is modeled by the following equation.

$$Wprd_{l,prd,t} = \sum_{lp \in Lcus} Ftrn_{l,lp,prd,t}, \quad \forall\, l \in Bio,\ prd,\ t \tag{14}$$

where $Ftrn_{l,lp,prd,t}$ is the amount of biofuel product prd shipped from algal biorefinery l to biofuel terminals ($lp \in Lcus$) in time period t.

Supercritical CO_2 Pipelines. We define a binary variable $Xp_{l,lp,t,mds}$, which is equal to 1 if there is a flow in the pipeline from node l to node lp in time period t and operating mode mds. This is modeled by the following equation.

$$Qcd_{l,lp,t,mds} \le qm_{l,lp} \cdot Xp_{l,lp,t,mds}, \quad \forall\, l,\ lp \in Adj_l,\ t,\ mds \tag{15}$$

where $qm_{l,lp}$ is the maximum possible flow rate between locations l and lp.

The following constraint indicates that only one pipeline with one diameter size can be installed on a certain arc. This is known as the single pipeline constraint.[21]

$$\sum_{dia} Yp_{l,lp,dia} \le 1, \quad \forall\, l,\ lp \in Adj_l \tag{16}$$

where $Yp_{l,lp,dia}$ is a binary variable, which is equal to 1 if a supercritical CO_2 pipeline with diameter dia is installed between nodes l and lp. Without loss of generality, we assume that there are no CO_2 pipelines between the nodes. Nevertheless, in cases that existing pipeline networks can be used, significant costs in capital investment can be saved. This can be easily accommodated in the proposed model by setting $Yp_{l,lp,dia}$ of the corresponding arc to 1.

Once the pipeline of a certain diameter is installed, the mass flow rate of supercritical CO_2 should be restricted within certain upper (q_{dia}^U) and lower (q_{dia}^L) bounds due to considerations of pressure drop, erosion speed, etc. This is modeled by introducing an auxiliary variable $Zp_{l,lp,dia,t,mds}$, which is equal to 1 if there is a positive flow in the pipeline from node l to lp with diameter dia in time period t and operating mode mds.

DOI: 10.1021/sc5008253
ACS Sustainable Chem. Eng. 2015, 3, 841−861

$$Qcd_{l,lp,t,mds} \le \sum_{dia} q^{U}_{dia} \cdot Zp_{l,lp,dia,t,mds}, \quad \forall\, l, lp \in Adj_l, t, mds \tag{17}$$

$$Qcd_{l,lp,t,mds} \ge \sum_{dia} q^{L}_{dia} \cdot Zp_{l,lp,dia,t,mds}, \quad \forall\, l, lp \in Adj_l, t, mds \tag{18}$$

Note that $Zp_{l,lp,dia,t,mds}$ is defined as a continuous variable between 0 and 1 in order to reduce the number of discrete variables in the model, whereas its combinatorial feature is accomplished using the following logic constraints.

$$Zp_{l,lp,dia,t,mds} \le Xp_{l,lp,t,mds}, \quad \forall\, l, lp \in Adj_l, dia, t, mds \tag{19}$$

$$Zp_{l,lp,dia,t,mds} \le Yp_{l,lp,dia}, \quad \forall\, l, lp \in Adj_l, dia, t, mds \tag{20}$$

$$1 + Zp_{l,lp,dia,t,mds} \ge Xp_{l,lp,t,mds} + Yp_{l,lp,dia}, \quad \forall\, l, lp \in Adj_l, dia, t, mds \tag{21}$$

Constraints 19 and 20 force $Zp_{l,lp,dia,t,mds}$ to be 0 if the pipeline is not operating in time period t in operating mode mds ($Xp_{l,lp,t,mds} = 0$) or if the pipeline with diameter dia is not installed ($Yp_{l,lp,dia} = 0$). When $Xp_{l,lp,t,mds}$ and $Yp_{l,lp,dia}$ are both equal to 1, constraint 21 would force $Zp_{l,lp,dia,t,mds}$ to be equal to 1.

Feed Gas Pipelines. The following constraints on feed gas pipelines are very similar to those on supercritical CO_2 pipelines; thus, they will not be explained one by one. It is worth pointing out that CO_2 is just one of the components in feed gas. Therefore, the mass flow rate of CO_2 is divided by the weight fraction (wf) to calculate the mass flow rate of feed gas in pipeline sizing constraints 24 and 25.

$$Qgcd_{l,lp,t,mds} \le qm_{l,lp} \cdot Xpg_{l,lp,t,mds}, \quad \forall\, l, lp \in Nbr_l, t, mds \tag{22}$$

$$\sum_{diag} Ypg_{l,lp,dia} \le 1, \quad \forall\, l, lp \in Nbr_l \tag{23}$$

$$\frac{Qgcd_{l,lp,t,mds}}{wf} \le \sum_{diag} qg^{U}_{diag} \cdot Zpg_{l,lp,dia,t,mds}, \quad \forall\, l, lp \in Nbr_l, t, mds \tag{24}$$

$$\frac{Qgcd_{l,lp,t,mds}}{wf} \ge \sum_{diag} qg^{L}_{diag} \cdot Zpg_{l,lp,dia,t,mds}, \quad \forall\, l, lp \in Nbr_l, t, mds \tag{25}$$

$$Zpg_{l,lp,diag,t,mds} \le Xpg_{l,lp,t,mds}, \quad \forall\, l, lp \in Nbr_l, diag, t, mds \tag{26}$$

$$Zpg_{l,lp,diag,t,mds} \le Ypg_{l,lp,diag}, \quad \forall\, l, lp \in Nbr_l, diag, t, mds \tag{27}$$

$$1 + Zpg_{l,lp,diag,t,mds} \ge Xpg_{l,lp,t,mds} + Ypg_{l,lp,diag}, \quad \forall\, l, lp \in Nbr_l, diag, t, mds \tag{28}$$

Biofuel Transportation. The amount of biofuels transported cannot exceed the capacity of the corresponding link.

$$Ftrn_{l,lp,prd,t} \le ftrn^{U}_{l,lp,prd,t}, \quad \forall\, l \in Bio, lp \in Lcus, prd, t \tag{29}$$

where $ftrn^{U}_{l,lp,prd,t}$ is the transportation capacity of biofuel prd from algal biorefinery l to biofuel terminal lp in time period t.

Biofuel Terminals. The total amount of product prd shipped from different algal biorefineries in time period t are sold at biofuel terminals in the same time period.

$$\sum_{l \in Bio} Ftrn_{l,lp,prd,t} = Sales_{lp,prd,t}, \quad \forall\, lp \in Lcus, prd, t \tag{30}$$

where $Sales_{lp,prd,t}$ is the sales amount of product prd sold at biofuel terminal lp in time period t.

The sales amount at a certain biofuel terminal must satisfy the demand lower bound ($dm^{L}_{l,prd,t}$) and cannot exceed the demand upper bound ($dm^{U}_{l,prd,t}$).

$$dm^{L}_{l,prd,t} \le Sales_{l,prd,t} \le dm^{U}_{l,prd,t}, \quad \forall\, l \in Lcus, prd, t \tag{31}$$

Economic Objective. The economic objective is to minimize the annualized total cost of the integrated CCUS supply chain, which includes the on-site carbon capture cost ($C^{capture}$), pipeline construction cost ($C^{pipe\_capital}$), pipeline operating and maintenance (O&M) cost (C^{pipe_om}), sequestration cost ($C^{sequestration}$), product distribution cost ($C^{distribution}$), and annualized cost of algal biorefineries (C^{bio}). The revenue from selling biofuel products ($C^{revenue}$) is counted as credit to mitigate the total cost.

$$C^{total} = C^{capture} + C^{pipe\_capital} + C^{pipe\_om} + C^{sequestration} + C^{distribution} + C^{bio} - C^{revenue} \tag{32}$$

The carbon capture cost is assumed to be proportional to the amount of CO_2 captured or retrieved. It includes the cost of cleanup, separation (only for CCS supply chain), and compression. The unit cost for carbon capture is denoted by c^{cap}_{l} while the unit cost for retrieving feed gas is denoted by cg^{cap}_{l}.

$$C^{capture} = \sum_{l \in Pow} \sum_{t} \sum_{mds} \tau_{t,mds} (c^{cap}_{l} \cdot Gcd_{l,t,mds} + cg^{cap}_{l} \cdot Ggcd_{l,t,mds}) \tag{33}$$

The pipeline construction cost is dependent on the selected pipeline diameter and the length of the pipeline network. The capital cost for installing a supercritical CO_2 pipeline from node l to node lp with diameter dia is denoted by $c^{pipe}_{l,lp,dia}$. The capital cost for installing a feed gas pipeline from node l to node lp with diameter $diag$ is denoted by $cg^{pipe}_{l,lp,diag}$. The construction cost is annualized by multiplying the annuity.

$$C^{pipe\_capital} = \frac{ir}{1 - (1 + ir)^{-ls}} \left(\sum_{dia} \sum_{l \in Pow} \sum_{lp \in Adj_l} c^{pipe}_{l,lp,dia} \cdot Yp_{l,lp,dia} + \sum_{diag} \sum_{l \in Pow} \sum_{lp \in Nbr_l} cg^{pipe}_{l,lp,diag} \cdot Ypg_{l,lp,diag} \right) \tag{34}$$

DOI: 10.1021/sc5008253
ACS Sustainable Chem. Eng. 2015, 3, 841−861

where *ir* is the annual discount rate, and *ls* is the lifetime of infrastructure in terms of years.

The pipeline O&M cost covers the costs for monitoring, scheduling, maintenance, etc. The O&M cost per unit pipeline length is denoted by $v^{pipe}_{l,lp,dia}$ and $vg^{pipe}_{l,lp,diag}$ for supercritical CO_2 pipelines and feed gas pipelines, respectively.

$$C^{pipe\_om} = \sum_{l\in Pow}\sum_{lp\in Adj_l}\sum_{dia}(v^{pipe}_{l,lp,dia}\cdot dis_{l,lp}\cdot Yp_{l,lp,dia}) + \sum_{l\in Pow}\sum_{lp\in Nbr_l}\sum_{diag}(vg^{pipe}_{l,lp,diag}\cdot dis_{l,lp}\cdot Ypg_{l,lp,diag}) \quad (35)$$

where $dis_{l,lp}$ is the distance from node l to lp.

The sequestration cost primarily includes the costs for injecting supercritical CO_2 underground and site monitoring. The unit sequestration cost is denoted by $c^{sink}_{l,t}$.

$$C^{sequestration} = \sum_{l\in \sin k}\sum_{t}\sum_{mds} c^{\sin k}_{l,t}\cdot\tau_{t,mds}\cdot Scd_{l,t,mds} \quad (36)$$

The product distribution cost covers the loading, unloading and shipping of biofuel products from algal biorefineries to biofuel terminals.

$$C^{distribution} = \sum_{l\in Bio}\sum_{lp\in Lcus}\sum_{prd}\sum_{t} c^{dist}_{l,lp,prd}\cdot Ftrn_{l,lp,prd,t} \quad (37)$$

where $c^{dist}_{l,lp,prd}$ is the unit distribution cost, which is dependent on the shipping distance.

The annualized cost of algal biorefineries includes annualized capital investments and O&M costs.

$$C^{bio} = \sum_{l\in Bio} Nc_l^{(p)} \quad (38)$$

where $Nc_l^{(p)}$ is an interface variable indicating the annualized cost of a certain algal biorefinery *l*. Detailed calculations for this cost can be found in the process model in Appendix A.

Revenue from selling the produced renewable biofuels includes two parts. One is from the market price ($price_{l,prd,t}$), and the other is from the volumetric incentive ($inct_{prd}$) provided by the government.

$$C^{revenue} = \sum_{l\in Lcus}\sum_{t}\sum_{prd}(price_{l,prd,t} + inct_{prd})\cdot Sales_{l,prd,t} \quad (39)$$

Environmental Objective. The environmental objective is to maximize the amount of GHGs avoided from entering the atmosphere, as shown by eq 40. The amount of CO_2 injected into the geological sinks is considered to be permanently removed from the atmosphere. The amount of CO_2 consumed at algal biorefineries is considered to be fixated in the biofuels produced. The net positive GHG emissions throughout the life cycle stages of the supply chain include emissions from carbon capture ($E^{capture}$), pipeline transportation (E^{pipe}), biofuel production (E^{bio}), and CO_2 injection at geological sinks ($E^{injection}$). The GHG emissions credit from producing renewable biofuels (E^{credit}) is also accounted for. Because all environmental parameters are given in terms of GWP, each of the terms in E^{total} has accounted for the aggregation of GHGs according to GWP.

$$E^{total} = -\sum_{l\in sink}\sum_{t}\sum_{mds}\tau_{t,mds}\cdot Scd_{l,t,mds} - \sum_{l\in Bio}\sum_{t}\sum_{mds}\tau_{t,mds}\cdot Hcd_{l,t,mds} + E^{capture} + E^{pipe} + E^{bio} + E^{distribution} + E^{injection} - E^{credit} \quad (40)$$

Carbon capture and separation processes can be very energy-consuming, so it must be considered in the life cycle analysis.

$$E^{capture} = \sum_{l\in Pow}\sum_{t}\sum_{mds}\tau_{t,mds}(e^{cap}_{l}\cdot Gcd_{l,t,mds} + eg^{cap}_{l}\cdot Ggcd_{l,t,mds}) \quad (41)$$

The transportation of supercritical CO_2 and feed gas requires the use of electricity to drive the pumps or compressors to maintain the desirable pressure and flow rate. We assume that the associated GHG emissions are proportional to the distance of transportation and mass flow rate.

$$E^{pipe} = \sum_{l\in Pow}\sum_{lp\in Adj_l}\sum_{t}\sum_{mds}(\tau_{t,mds}\cdot e^{pipe}_{l,lp}\cdot dis_{l,lp}\cdot Qcd_{l,lp,t,mds}) + \sum_{l\in Pow}\sum_{lp\in Nbr_l}\sum_{t}\sum_{mds}(\tau_{t,mds}\cdot eg^{pipe}_{l,lp}\cdot dis_{l,lp}\cdot Qgcd_{l,lp,t,mds}) \quad (42)$$

The GHG emissions at algal biorefineries primarily come from the use of electricity, heat, and consumables. The GHG emissions corresponding to each conversion route are quantified in the process model.

$$E^{bio} = \sum_{l\in Bio} Gwp_l^{(p)} \quad (43)$$

The GHG emissions in biofuel distribution are largely due to the use of liquid transportation fuels, which relates to the transportation distance and load of shipment. We assume that the trucks run on conventional transportation fuels.

$$E^{distribution} = \sum_{l\in Bio}\sum_{lp\in Lcus}\sum_{prd}\sum_{t} e^{dist}_{l,lp,prd}\cdot Ftrn_{l,lp,prd,t} \quad (44)$$

The injection process also consumes energy, which is assumed to be proportional to the amount of supercritical CO_2 injected.

$$E^{injection} = \sum_{l\in sink}\sum_{t}\sum_{mds} e^{inj}_{l,t}\cdot\tau_{t,mds}\cdot Scd_{l,t,mds} \quad (45)$$

The produced renewable biofuels can displace their petroleum counterparts in the marketplace. Therefore, by using the produced renewable biofuels, the life cycle emissions associated with the production, transportation, and combustion of the same amount of petroleum-derived liquid transportation fuels can be avoided, which are considered as environmental credit in the CCUS supply chain.

$$E^{credit} = \sum_{l\in Lcus}\sum_{t}\sum_{prd} e^{displace}_{prd}\cdot Sales_{l,prd,t} \quad (46)$$

We note that the above model is a multiobjective nonconvex MINLP problem. It includes an economic objective 32 and an environmental objective 40. Nonlinearities come from the process model, where the capital costs of the processes are calculated as concave functions with respect to the capacities

DOI: 10.1021/sc5008253
ACS Sustainable Chem. Eng. 2015, 3, 841−861

(eq A.20). To solve this problem effectively, we present solution strategies in the following section.

SOLUTION STRATEGIES

Because we have two objective functions in the above model, multiobjective solution techniques are required according to the LCO framework. We adopt the standard ε-constraint method in this work and transform the environmental objective into the following ε-constraint.

$$E^{total} \geq \varepsilon \tag{47}$$

The resulting model is a single-objective MINLP that minimizes the total annualized cost for CO_2 reduction subject to the ε-constraint on GHG abatement. By setting the parameter ε to different values and solving the MINLP, we can obtain a sequence of Pareto-optimal solutions, which would reveal the trade-off between the economic and environmental objectives.

Although off-the-shelf global optimizers (e.g., BARON 14,[71] SCIP 3) can be used to solve the MINLP problem presented above, they usually require a considerable amount of computational time and resources due to the combinatorial nature and nonconvexity of the model.[72,73] To further facilitate the solution, we employ an improved branch-and-refine algorithm in this work. The algorithm takes advantage of powerful MILP solvers (e.g., CPLEX 12) and returns the global optimal solution to the nonconvex MINLP problem by solving a sequence of MILP subproblems.[74,75] These MILP problems are convex relaxations of the original MINLP, which are constructed successively as the branch-and-refine algorithm proceeds based on the piecewise linear approximations of the concave terms.[76] There are several alternative formulations to construct the piecewise linear approximations.[77] We employ the SOS1 formulation in this work because it has been shown to be the most efficient formulation.[78,79] It is apparent that the finer the grid partitioning is, the smaller the approximation error is. However, the best partitioning scheme is not known beforehand. By using this improved branch-and-refine algorithm, we can automatically determine the addition of grid points and effectively converge to the global optimal solution within finite iterations.[80] The procedure of this improved branch-and-refine algorithm is shown in Figure 4 and is based on the work by Bergamini et al.[81]

STATEWIDE CASE STUDY

In this section, we present a statewide case study on the optimal design and planning of a CCUS supply chain network in Texas.[82] There are three reasons that we chose Texas for this case study. First, a significant portion of electricity supply in Texas is generated from coal-fired power plants,[83] which are the biggest source of anthropogenic CO_2 emissions. Second, there are a number of enhanced oil recovery fields and saline aquifers in western Texas, which provide sufficient capacity for carbon storage.[84] Third, the climate (e.g., temperature, insolation) and geological factors (e.g., land, water) in Texas are favorable for commercial-scale algal biofuel production.[47]

We plot all of the potential facilities involved in the integrated CCUS infrastructure in Figure 5, including five existing power plants (i.e., red squares), one geological sink (i.e., orange triangle), five candidate sites for building algal biorefineries (i.e., green stars), and seven biofuel terminals (i.e., blue dots). The background is the terrain map of Texas.[85] The

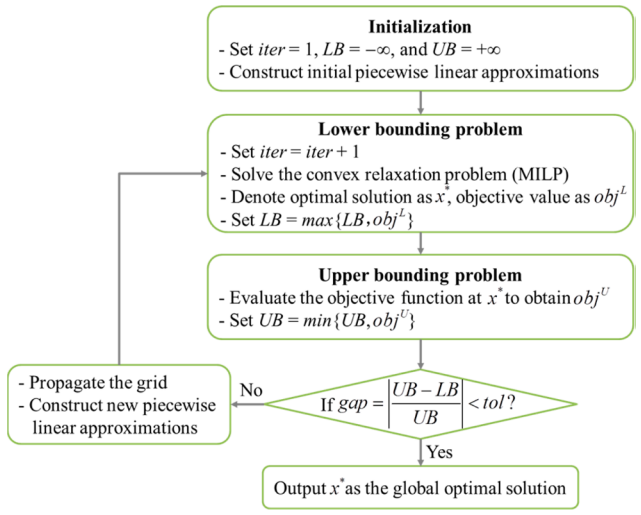

Figure 4. Flowchart of the branch-and-refine algorithm.

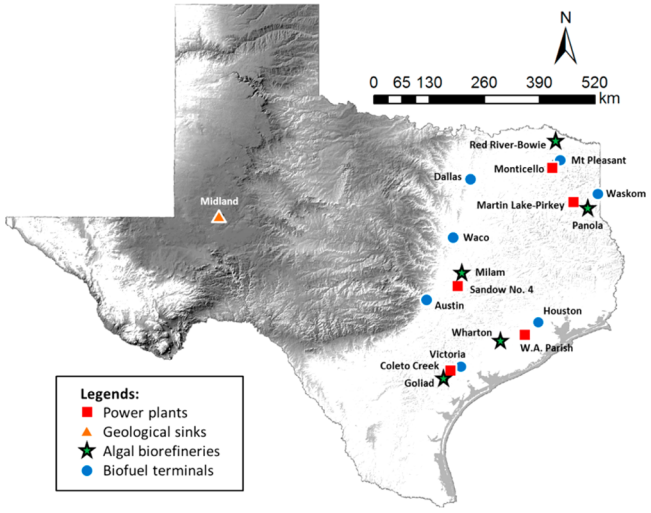

Figure 5. Facility locations in the region under consideration: Texas.

power plants are selected from the potential retrofit candidates for carbon capture identified by the Nicholas Institute's version of the U.S. Energy Information Agency's National Energy Modeling System (NI-NEMS).[82] According to the work by Zhou and Pratson,[86] Midland is chosen as the only geological sink in this case study. The selection of candidate sites for algal biorefineries is based on the work by Venteris et al.,[48] which considered both water and land use factors. The authors identified a number of potential algal pond sites that would discharge less than 5% of the freshwater supply in the corresponding watershed. We lump the adjacent sites and select the ones that are close to the selected power plants as our algal biorefinery candidate sites. Biofuel terminals might have demand for biodiesel, renewable diesel, or both. The biodiesel terminals are chosen from existing biodiesel fueling stations published on the U.S. Department of Energy Web site.[87] Because renewable diesel is essentially the same in composition and function as petroleum-derived diesel, the renewable diesel terminals are chosen from the existing petroleum product terminals published on the U.S. Energy Information Administration Web site.[88] For each segment of supercritical CO_2 pipeline, there are nine sizes of pipelines to choose, with the nominal diameter ranging from 4 to 36 in. For each segment of

DOI: 10.1021/sc5008253
ACS Sustainable Chem. Eng. 2015, 3, 841−861

feed gas pipeline, there are six sizes of pipelines to choose, with the nominal diameter ranging from 48 to 108 in. The lower and upper bounds of mass flow rate corresponding to each size of pipeline are obtained from the literature or estimated using empirical equations.[22,89−91] More information about the facilities and pipelines can be found in Appendix B.

Policies on the CO_2 emissions reduction target have a significant impact on the power sector.[6] A relatively low reduction target (e.g., 20%) can be achieved through increased efficiency and fuel switching. However, a high reduction target for coal-fired power plants calls for the use of CCS and CU technologies.[31,92] The annual CO_2 reduction target is set to 80% for all coal-fired power plants. The loss factor during carbon capture or feed gas retrieval is assumed to be 10%, so at most 90% of the CO_2 emissions can be sequestrated and utilized.[39] We project the life span of the integrated CCUS infrastructure to be 20 years, and an annual discount rate of 10% is considered. To capture seasonality of operations, we divide a year into 12 time periods (i.e., one month per time period). CO_2 emissions from the power plants in each time period are assumed to be proportional to electricity consumption in the same period, projected from historical data.[93] The lower bounds of biofuel consumption at the biofuel terminals are set to zero, and the upper bounds are set to a sufficiently large value, assuming that all biofuels produced can be consumed. According to a report by U.S. Department of Energy, prices for biodiesel and renewable diesel in the Gulf Coast area are at $3.70 and $3.77 per gallon, respectively (average price in July, 2014).[94] We assume a volumetric incentive of $1.00 per gallon for both biodiesel and renewable diesel.[95] In each period, we consider two operating modes, namely, daytime and nighttime. We collected data on the length of daytime[96] and solar irradiation[97] in each month of the year to calculate the varying productivity of algal biomass and biofuels throughout the year. It is assumed that algal biorefineries do not consume CO_2 during nighttime production, but the biofuel production processes can operate continuously.[50] This is accomplished by adding biomass storage tanks so that the surplus algal biomass produced during the daytime operation can be processed at night. The techno-economic and emissions data associated with each technology involved in the processing network can be found in the work by Gong et al.[50] The process model employed in this work is adapted from the MINLP model proposed in the same work by adding indices of time periods and locations, as well as capacity variables. The capital and operations and maintenance (O&M) costs of supercritical CO_2 pipelines are calculated using the formula provided by the National Energy Technology Laboratory (NETL), which are dependent on the length and diameter of the pipeline.[98] The capital and O&M costs of feed gas pipelines are also calculated using the same formula. However, due to lower pressures in feed gas pipelines, the wall thickness of feed gas pipelines can be smaller than that of supercritical CO_2 pipelines. Thus, as suggested by NETL, we decrease the costs of feed gas pipelines by a factor of 25%.[99] The great circle distances between the locations are calculated using the Haversine formula using longitude and latitude information.[69] Truck transportation is considered for shipping biofuels from algal biorefineries to biofuel terminals. The GHG emissions associated with carbon capture, transportation, and sequestration are estimated from the literature.[100−102] GHG emissions data associated with other life cycle stages of the supply chain are obtained from the EcoInvent database[66] and GREET model.[103]

All computational experiments are performed on a PC with an Intel Core i5-2400 CPU @ 3.10 GHz and 8.00 GB RAM. All models and solution procedures are coded in GAMS 24.3.3. The MILP subproblems involved in the branch-and-refine algorithm are solved with CPLEX 12. The MINLP problems are solved with BARON 14[71] or SCIP 3. The relative optimality criteria for all the solvers are set to 1%. The tolerance of the gap between the upper and lower bounds in the branch-and-refine algorithm is set to 1%.

Pareto Curve. As aforementioned, the proposed multi-objective MINLP model is tackled by ε-constraint method. We set the ε-parameter to 10 values evenly distributed between the lower and upper bounds of the environmental objective, i.e., from 16.688 to 21.277 Mt CO_2-equivalent of GHGs avoided per year. The resulting Pareto-optimal solutions are plotted in Figure 6.

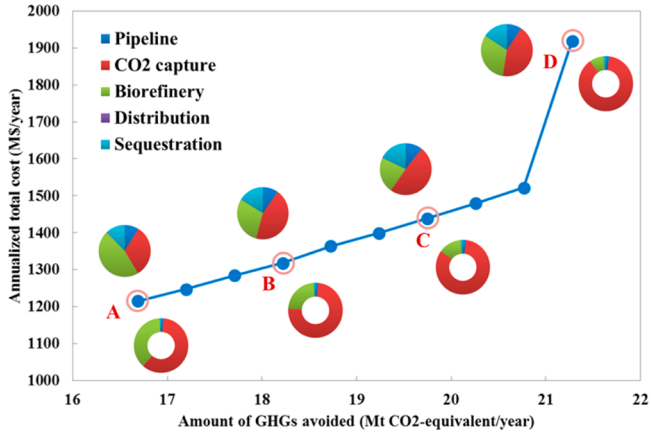

Figure 6. Pareto curve of the case study with breakdown of the cost and emissions. Pie charts represent cost breakdowns. Doughnut charts represent emissions breakdowns.

These 10 Pareto-optimal solutions constitute an approximated Pareto curve. The solutions above this curve are suboptimal, while the solutions below this curve are infeasible. The abscissa represents the amount of GHGs avoided from entering the atmosphere with the deployment of the CCUS project, and the ordinate represents the annualized total cost of the CCUS project. It can be seen that as the requirement on the amount of GHGs avoided from entering the atmosphere increases from 16.688 to 21.277 Mt CO_2-equivalent/year, the annualized total cost of the project increases from 1.22 to 1.92 billion dollars. Although all of the solutions on this Pareto curve are considered optimal, their focus with respect to the economic and environmental performances varies. Points on the right tend to maximize the GHGs abatement effect, while points on the left tend to pursue a more cost-effective supply chain. We also present the costs and emissions breakdowns for selected points on the Pareto curve. The pie charts above the Pareto curve correspond to the cost breakdowns. As shown, the primary costs come from the capital and O&M costs of algal biorefineries and CO_2 capture. Overall, as the requirement on the amount of GHGs avoided increases, the portion of CO_2 capture cost increases. Regarding the GHG emissions, the storage, utilization, and fossil fuel substitution effect are considered to be (negative) credits, but the net positive

DOI: 10.1021/sc5008253
ACS Sustainable Chem. Eng. 2015, 3, 841−861

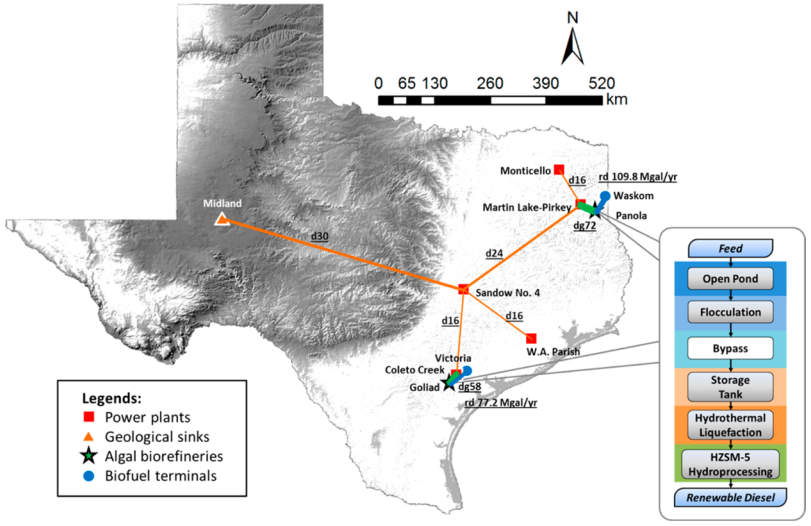

Figure 7. Optimal supply chain design of the most cost-effective solution.

GHG emissions also deserve our attention. The doughnut charts below the Pareto curve correspond to emissions breakdowns. As shown, the primary positive emissions in the supply chain come from the operations of CO_2 capture and algal biorefineries. As the requirement on the amount of GHGs avoided increases, the portion of CO_2 capture emissions increases.

There are two points in particular that deserve our attention. The point on the lower left (A) of the curve has the lowest annualized total cost, and it is therefore the most cost-effective supply chain design. On the other hand, the point on the upper right of the curve (D) leads to the maximum GHGs abatement effect, and it is therefore the most environmentally sustainable solution. We will look into these solutions in more detail in the following sections.

Most Cost-Effective solution. Figure 7 shows the supply chain design of the most cost-effective solution. We have removed the inactive nodes from the map. The supercritical CO_2 pipelines are denoted by orange lines. The thickness of the line indicates the nominal diameter of the pipelines, and the underlined number next to the line indicates the exact value of the nominal diameter (e.g., d16 refers to the supercritical CO_2 pipeline with a nominal diameter of 16 in.). The feed gas pipelines are denoted by green lines. Similarly, the thickness of the line indicates the nominal diameters of the pipelines, and the underlined number next to the line indicates the exact value of the nominal diameter (e.g., dg58 refers to the feed gas pipeline with a nominal diameter of 58 in.). The blue lines indicate that biofuels are shipped in the corresponding links. The thickness of the line indicates the annual transportation level of algal biofuels, and the underlined number next to the line indicates the exact value of the shipment load (where rd refers to renewable diesel and bd refers to biodiesel). We can see that both the geological sequestration and microalgae biofixation options are employed. This is because the microalgae biofixation option alone is not adequate to reach the 80% CO_2 reduction target at the power plants because algal biorefineries cannot utilize CO_2 emissions during the nighttime production. On the other hand, this result shows that taking advantage of the synergies between both options leads to a lower CO_2 reduction cost compared to using the geological sequestration option alone. Instead of transporting supercritical CO_2 to the geological sink from individual power plants directly, the supercritical CO_2 streams from different power plants are gathered at the Sandow No. 4 power plant and transported to Midland using a 30 in. trunkline to reduce pipeline construction and operations costs. Two algal biorefineries are installed in Panola and Goliad County. The Panola biorefinery utilizes the feed gas from the Martin Lake − Pirkey power plant, and the Goliad biorefinery utilizes the feed gas from the Coleto Creek power plant. Renewable diesel is produced at both algal biorefineries using the optimal route shown on the right of Figure 7. This route has a higher biomass-to-biofuel conversion efficiency, but it is also energy intensive, leading to relatively higher indirect GHG emissions compared to other routes. The renewable biodiesel produced at the Panola and Goliad biorefineries is shipped to the closest biofuel terminal that has demand for renewable diesel—the Waskom and Victoria terminals, respectively. Waskom consumes 109.8 M gallon of renewable diesel per year, and Victoria consumes 77.2 M gallon of renewable diesel per year. To investigate how the CO_2 emissions are used, in Figure 8, we

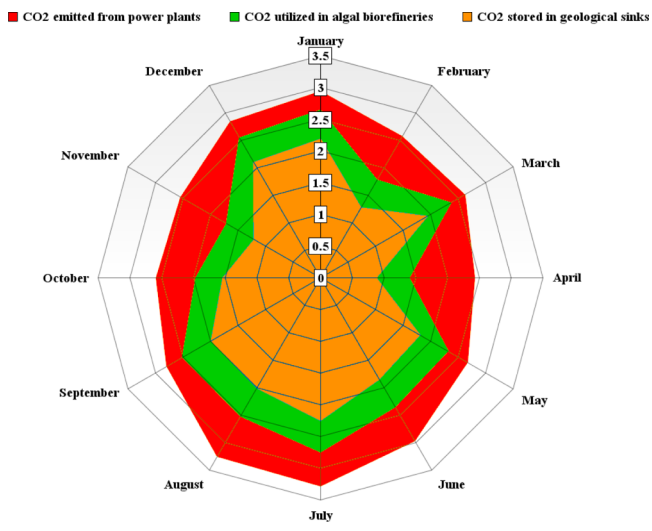

Figure 8. CO_2 emissions, usage, and storage in the most cost-effective solution (unit: Mt CO_2).

DOI: 10.1021/sc5008253
ACS Sustainable Chem. Eng. 2015, 3, 841−861

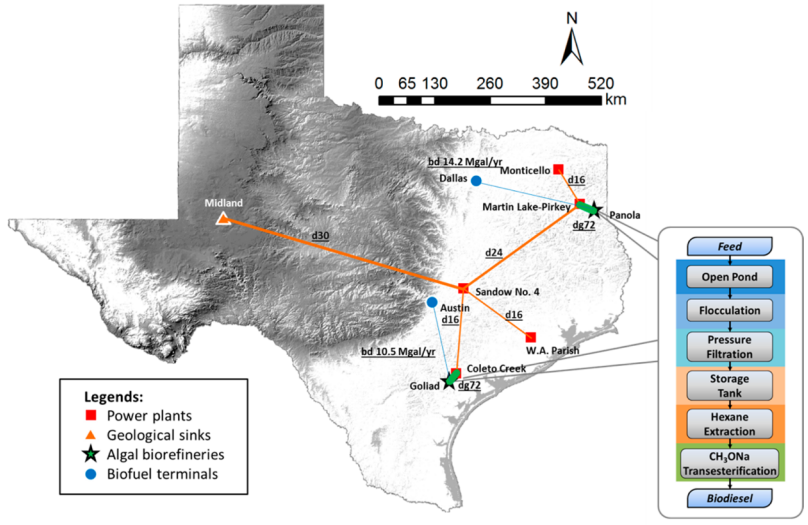

Figure 9. Optimal supply chain design of the most environmentally sustainable solution.

plot the amount of CO_2 emitted from the power plants (red part), utilized by the algal biorefineries (green part), and injected into the geological sinks (orange part) in each time period as a radar chart. The sum of the amount of CO_2 utilized and stored is equal to 80% of the total CO_2 emissions so that the 80% CO_2 annual reduction target at the power plants is met. We note that there are many factors influencing the use of CO_2 emissions, including variations in electricity supply, length of daytime, and biomass productivity, as well as process capacity of the installed algal biorefineries. As given, the total amount of CO_2 emissions from all power plants is 33.384 Mt CO_2/year, so 30.029 Mt CO_2 is sequestrated and utilized through the CCUS supply chain every year. Because the annualized cost of the project is 1.22 billion dollars, this indicates that the CO_2 emissions can be sequestrated and utilized at an average cost of \$45.52/tCO_2.

Most Environmentally Sustainable Solution. Figure 9 shows the supply chain design of the most environmentally sustainable solution. The CCS pipeline network is the same as that of the most cost-effective solution because using the minimum length of supercritical CO_2 pipelines also helps reduce the indirect GHG emissions associated with operation of the pipelines. Again, the Panola and Goliad biorefineries are installed. However, the feed gas flow rate from the Coleto Creek power plant to the Goliad biorefinery is higher, as a 72 in. pipeline is used instead of a 58 in. one. Furthermore, biodiesel instead of renewable diesel is produced at both the Panola and Goliad biorefinery and shipped to the closest biofuel terminals that have demand for biodiesel—the Dallas and Austin terminals, respectively. Dallas consumes 14.2 M gallon of biodiesel per year, and Austin consumes 10.5 M gallon of biodiesel per year. The optimal route selected in both algal refineries is shown on the right of Figure 9. This route is chosen because it has the lowest environmental impact compared to other routes. We can see how the CO_2 emissions are used in the radar chart in Figure 10. The sum of the amount of CO_2 stored and utilized is equal to 90% of the total CO_2 emissions from the power plants, which is the presumed maximum amount that can be captured or retrieved due to the losses of flue gas and technology limitations. We can see that CO_2 emissions are only utilized in the algal biorefineries from April to September because the length of daytime and biomass

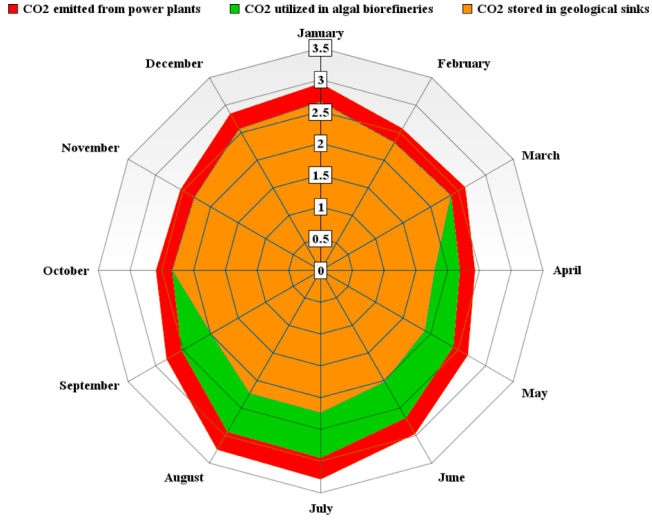

Figure 10. CO_2 emissions, usage, and storage in the most environmentally sustainable solution (unit: Mt CO_2).

productivity are more favorable for biodiesel production in these time periods. As given, the total amount of CO_2 emissions from all of the power plants is 33.384 Mt CO_2/year. In the most environmentally sustainable solution, the total amount of GHGs avoided from entering the atmosphere is 21.277 Mt CO_2-equivalent. Therefore, about 64% of GHGs are avoided.

Computational Performance. It takes about a total of 70 h (CPU time) to obtain all 10 Pareto-optimal solutions using the branch-and-refine algorithm. To demonstrate the performance of the branch-and-refine algorithm, we also solve the nonconvex MINLP problem corresponding to the most cost-effective solution with BARON 14 and SCIP 3 for comparison. This MINLP problem has 256 discrete variables, 2,011,081 continuous variables, and 2,398,620 constraints. The computational performances of different solution methods are presented in Table 1.

We can see that the branch-and-refine algorithm converges to the globally optimal solution in less than 2 h and after five iterations. In contrast, both global optimizers fail to converge within the 20 h limit. BARON 14 fails to return any solution

DOI: 10.1021/sc5008253
ACS Sustainable Chem. Eng. 2015, 3, 841−861

Table 1. Computational Performances of Different Solution Methods

Solution method	Lower bound (M$/year)	Upper bound (M$/year)	Relative gap	Iteration	Solution time (CPUs)
BARON 14	–	–	–	–	720,000[a]
SCIP 3	1,024.123	1,231.673	20.27%	–	720,000[b]
Branch-and-refine	1,214.851	1,215.620	<1%	5	6,607

[a]No solution returned within 720,000 s (20 h). [b]Computation time limit reached.

after 20 h. SCIP 3 returns valid lower and upper bounds, but the relative gap is still significant after 20 h of solution time. Therefore, it is shown that the branch-and-refine algorithm is much more efficient in solving the resulting nonconvex MINLP problem.

CONCLUSIONS

We proposed a novel MINLP model for the optimal design and operations of integrated CCUS supply chains. We simultaneously considered two options for GHG abatement, namely, geological sequestration and microalgae biofixation. In the former option, CO_2 is captured and separated at power plants and then transported to geological sinks via supercritical CO_2 pipelines for underground injection. In the latter option, CO_2 is preprocessed at power plants and then transported as a component of feed gas via pipelines to nearby algal biorefineries to serve as the primary nutrition for algae growth. A detailed process model was employed for the design of algal biorefineries, which involved 13 potential routes for converting algal biomass into biofuels. The incorporation of this detailed process model into a supply chain network model improved the modeling fidelity and led to vertical integration across different scales. The seasonalities in CO_2 availability at power plants and algae productivity at algal biorefineries were modeled by a multiperiod optimization formulation, which enabled us to capture the operational variations at different times of a year. To reveal the trade-off between different supply chain design options under economic and environmental criteria, we applied the LCO framework by optimizing two objectives simultaneously. The economic objective is minimizing the total cost for reaching specified CO_2 reduction targets at power plants. The environmental objective is maximizing the total amount of GHG avoided from entering the atmosphere considering all life cycle stages of the supply chain. The application of this model was illustrated by a statewide case study in Texas. Results showed that CCS through the geological sequestration option is necessary for reaching the 80% CO_2 reduction target. Producing and selling biofuels through the microalgae biofixation option in concert with CCS can help reduce the CO_2 reduction cost and improve the GHG abatement effect. Producing renewable diesel has the largest cost saving potential, whereas producing biodiesel avoids more GHGs from entering the atmosphere.

APPENDIX A: PROCESS MODEL

We present the detailed process model for the conversion pathway selection in this section. The model is adapted from Gong et al.[50] by adding indices of time periods and locations, as well as variables on process capacities.

Mass Balance Constraints

The mass balance constraints are divided into two groups. The first group describes the configuration of the algal biorefinery with binary variables and logic constraints. The second group establishes a general mass balance framework for each technology.

Superstructure Configuration Constraints. Equations A.1 and A.2 describe the configuration of the proposed superstructure. We introduce a binary variable $Y_{l,i,j}$ to model the selection of technology j of section i in location l. If the technology is selected, $Y_{l,i,j}$ equals 1; otherwise, $Y_{l,i,j}$ equals 0. Determined by binary variable Xb_l, eq A.1 guarantees at most one technology j among the available alternatives in section i is selected if a biorefinery is built in location l; otherwise, no technology in location l is activated.

$$\sum_{j\in J} Y_{l,i,j} \le 1, \quad \forall\, l \in L,\ i \in I \tag{A.1}$$

$$0 \le Mc^{n}_{l,i,j,k} \le Y_{l,i,j}\cdot ub, \quad \forall\, l \in L,\ i \in I,\ j \in J,\ k \in K,\ n \in N \tag{A.2}$$

Constraint A.2 provides the lower and upper bounds of the capacity $Mc^{n}_{t,l,i,j,k}$ of species k in flow n of technology j of section i in location l. In this constraint, ub is the upper bound of the mass flow rate; superscript n represents the flows involved in the general mass balance framework. The upper bound of the mass flow rate is estimated to be 10^8 t/h by postulating an open pond cultivation system and a transesterification process for biodiesel production. Note that if a technology is bypassed, its binary variable will be equal to 0, and the lower bounds and upper bounds will be constrained to 0 simultaneously, resulting in 0 for the corresponding mass flow rates.

General Mass Balance Framework. The general mass balance framework employs three sequential steps in the modeling of each technology. These steps include an inlet converging step, a conversion step, and an outlet separation step.

The inlet converging step, consisting of eqs A.3−A.6, prepares the input flow by integrating an "up" flow, a "reuse" flow, and a "makeup" flow. Before the details of each constraint are given, we declare i' and k' as aliases for i and k, respectively. Equation A.3 defines the total mass flow rate of species k in the "up" flow of section i in location l and time period t as the sum of corresponding "down" flows. D_i is the subset of sections whose "down" flows go to section i. Likewise, eq A.4 defines the "reuse" flow based on "recycle" flows, and R_i is the subset of sections whose "recycle" flows go to section i. $p^{in}_{i,j,k,k'}$ is the concentration of species k based on species k' in the "in" flow of technology j in section i. Equation A.6 defines the mass flow rate of the inlet flow $Mr^{in}_{t,l,i,j,k}$ by summing the corresponding "up", "reuse", and "makeup" flows.

$$\sum_{j\in J} Mr^{up}_{t,l,i,j,k} = \sum_{i'\in D_i, j\in J} Mr^{down}_{t,l,i',j,k}, \quad \forall\, t \in T,\ l \in L,\ i \in I,\ k \in K \tag{A.3}$$

DOI: 10.1021/sc5008253
ACS Sustainable Chem. Eng. 2015, 3, 841−861

$$\sum_{j\in J} Mr^{reuse}_{t,l,i,j,k} = \sum_{i'\in R_i, j\in J} Mr^{recycle}_{t,l,i',j,k},$$
$$\forall\, t\in T,\ l\in L,\ i\in I,\ k\in K \tag{A.4}$$

$$Mr^{in}_{t,l,i,j,k} = \sum_{k'\in K} (p^{in}_{i,j,k,k'}\cdot Mr^{in}_{t,l,i,j,k'}),$$
$$\forall\, t\in T,\ l\in L,\ i\in I,\ j\in J,\ k\in K \tag{A.5}$$

$$Mr^{in}_{t,l,i,j,k} = Mr^{up}_{t,l,i,j,k} + M^{reuse}_{t,l,i,j,k} + Mr^{makeup}_{t,l,i,j,k},$$
$$\forall\, t\in T,\ l\in L,\ i\in I,\ j\in J,\ k\in K \tag{A.6}$$

The conversion step is specified by eq A.7, which describes the chemical reaction occurring in the corresponding technology. $x_{t,i,j}$ is the reaction conversion of technology j in section i in time period t; $sc_{i,j,k,k'}$ is the stoichiometric coefficient of species k based on species k' in the reaction of technology j in section i.

$$Mr^{out}_{t.l,i,j,k} = Mr^{in}_{t,l,i,j,k} + \sum_{k'\in K} (sc_{i,j,k,k'}\cdot x_{t,i,j}\cdot Mr^{in}_{t,l,i,j,k'}),$$
$$\forall\, t\in T,\ l\in L,\ i\in I,\ j\in J,\ k\in K \tag{A.7}$$

Finally, the outlet separation step from eqs A.8−A.10 separates the reaction products into a "down" flow, a "recycle" flow, and an "emission" flow. As the separation equipment is already included in the technology box together with converging and conversion equipment, the split flows contain necessary fractions from the "out" flow. $sf^{down}_{i,j,k,k'}$ is the split fraction of species k of technology j in section i to the "down" flow on the basis of species k'; $sf^{emission}_{i,j,k}$ is the split fraction of species k of technology j in section i into the "emission" flow. Because the "out" flow is defined as the sum of these three flows, the remaining components stay in the corresponding "recycle" flow.

$$Mr^{out}_{t,l,i,j,k} = Mr^{down}_{t,l,i,j,k} + Mr^{recycle}_{t,l,i,j,k} + Mr^{emission}_{t,l,i,j,k},$$
$$\forall\, t\in T,\ l\in L,\ i\in I,\ j\in J,\ k\in K \tag{A.8}$$

$$Mr^{down}_{t,l,i,j,k} = \sum_{k'\in K} (sf^{down}_{i,j,k,k'}\cdot Mr^{out}_{t,l,i,j,k'}),$$
$$\forall\, t\in T,\ l\in L,\ i\in I,\ j\in J,\ k\in K \tag{A.9}$$

$$Mr^{emission}_{t,l,i,j,k} = sf^{emission}_{i,j,k}\cdot Mr^{out}_{t,l,i,j,k},$$
$$\forall\, t\in T,\ l\in L,\ i\in I,\ j\in J,\ k\in K \tag{A.10}$$

The highest flow rate $Mc^{n}_{l,i,j,k}$ is defined by eq A.11.

$$Mr^{n}_{t,l,i,j,k} \le Mc^{n}_{l,i,j,k},$$
$$\forall\, t\in T,\ l\in L,\ i\in I,\ j\in J,\ k\in K \tag{A.11}$$

The feedstock flows of the superstructure are defined by eq A.12. wf^{CO2}_{k} represents the weight fractions of the feed gas; $Hcd^{hr}_{l,t}$ is the total mass flow of the feed gas.

$$\sum_{j\in J} Mr^{up}_{t,l,cultivation,j,k} = wf^{CO2}_{k}\cdot Hcd^{hr}_{l,t},$$
$$\forall\, t\in T,\ l\in L,\ k\in K \tag{A.12}$$

Energy Balance Constraints

The energy balance of the proposed superstructure involves the conservation of electricity, heating, and cooling utilities. In each category, we calculate the amount of energy consumption and generation based on the mass flow rates.

Electricity. The electricity consumption of section i is modeled by eq A.13, where $upc_{i,j,k}$ is the unit power consumption of species k of technology j in the corresponding section.

$$Pcr_{t,l,i} = \sum_{j\in J,k\in K} (upc_{i,j,k}\cdot x_{t,i,j}\cdot Mr^{in}_{t,l,i,j,k}),$$
$$\forall\, t\in T,\ l\in L,\ i\in I \tag{A.13}$$

The total electricity consumption of the algal biorefinery is satisfied by directly purchasing electricity from the grid.

$$Npcr_{t,l} = \sum_{i\in I} Pcr_{t,l,i} - Ptr_{t,l},\qquad \forall\, t\in T,\ l\in L \tag{A.14}$$

The net electricity consumption is defined by eq A.14, where $Ptr_{t,l}$ represents the amount of electricity offset by the electricity supplies. The net electricity generation rate is defined by eq A.15, where $\eta^{turbine}$ denotes the energy conversion efficiency of the turbine, lhv_k represents the lower heating value of species k, and G is the subset of species that are the combustible gaseous components.

$$Nppr_{t,l} = \eta^{turbine}\cdot \sum_{k\in G} (lhv_k\cdot Mr^{in}_{t,l,elec-gen,turbine,k}) - Ptr_{t,l},$$
$$\forall\, t\in T,\ l\in L \tag{A.15}$$

Heating. The heating utility consumption and generation are defined by constraints A.16 and A.17 in a similar manner to electricity. $uhc_{i,j,k}$ is the unit heat consumption of species k of technology j in the corresponding section; Y^{he} and Y^{com} denote the energy conversion efficiency of the heat exchanger and combustor, respectively.

$$Hcr_{t,l,i} = \sum_{j\in J,k\in K} (uhc_{i,j,k}\cdot x_{t,i,j}\cdot Mr^{in}_{t,l,i,j,k}),$$
$$\forall\, t\in T,\ l\in L,\ i\in I \tag{A.16}$$

The net electricity consumption is defined by eq A.17.

$$Nhcr_{t,l} = \sum_{i\in I} Hcr_{t,l,i},\ \forall\, t\in T,\ l\in L \tag{A.17}$$

Cooling. The cooling utility balance is evaluated following the similar fashion of that for the heating utility and electricity as shown in eqs A.18 and A.19.

$$Ccr_{t,l,i} = \sum_{j\in J,k\in K} (ucc_{i,j,k}\cdot x_{t,i,j}\cdot Mr^{in}_{t,l,i,j,k}),$$
$$\forall\, t\in T,\ l\in L,\ i\in I \tag{A.18}$$

$$Nccr_{t,l} = \sum_{i\in I} Ccr_{t,l,i},\qquad \forall\, t\in T,\ l\in L \tag{A.19}$$

Economic Evaluation Constraints

The goal of economic evaluation is to identify the unit annualized cost including both capital and operating costs.

DOI: 10.1021/sc5008253
ACS Sustainable Chem. Eng. 2015, 3, 841−861

$$Cc_{l,i,j} = cc_{i,j}^{b}\left(\frac{M_{l,i,j}}{m_{i,j}^{b}}\right)^{sf_{i,j}}\left(\frac{cepci_{i,j}}{cepci_{i,j}^{b}}\right), \quad \forall\, l \in L,\ i \in I,\ j \in J \tag{A.20}$$

$$M_{l,i,j} = \sum_{k \in C_i} Mc_{l,i,j,k}^{in}, \quad \forall\, l \in L,\ i \in I,\ j \in J \tag{A.21}$$

The equipment capital cost is estimated by the sizing function in eq A.20, where $cc_{i,j}^{b}$ is the capital cost of technology j in section i in the base case; $m_{i,j}^{b}$ is the mass flow rate of technology j in section i in the base case; $sf_{i,j}$ is the sizing factor of technology j in section i. We note that the sizing factor $SF_{i,j}$ usually ranges from 0 to 1, resulting in a number of concave terms. Furthermore, we use the chemical engineering plant cost index of the reference year $cepci_{i,j}$ and of the base year $cepci_{i,j}^{b}$ to account for inflation. The mass flow rate of $M_{l,i,j}$ is defined by eq A.21, where C_i is the subset of species that contribute to $M_{l,i,j}$ in section i.

$$Lc_l = price^{land} \cdot Area_l, \quad \forall\, l \in L \tag{A.22}$$

$$Area_l = \frac{Mc_{l,cultivation,openpond,algae}^{out}}{pro}, \quad \forall\, l \in L \tag{A.23}$$

The land cost Lc_l of the algal biorefinery is evaluated by eq A.22, where $price^{land}$ is the unit land cost; $Area_l$ is the land area occupied by the open pond cultivation facilities; pro is the area productivity of the open pond in the cultivation section.

$$Tpic_l = p^{K} \cdot \sum_{i \in I, j \in J} Cc_{l,i,j} + Lc_l, \quad \forall\, l \in L \tag{A.24}$$

The total project investment cost in different location l, denoted *as* $Tpic_l$, is calculated by eq A.24 and accounts for equipment capital costs, field materials, and labor costs for installation, insurance, freight costs, construction costs, contractor engineering costs, and land costs. p^{K} is the total project investment cost multiplier based on the total capital cost. The annualized investment cost is calculated by eq A.25, where ir is the discount rate, and ls is the life span of this project in years.

$$Aic_l = Tpic_l \cdot \frac{ir \cdot (ir+1)^{ls}}{(ir+1)^{ls} - 1}, \quad \forall\, l \in L \tag{A.25}$$

The annual operating cost Aoc_l is quantified by eqs A.26–A.30 as the sum of feedstock cost, utility cost, O&M cost, and waste disposal cost. In these equations, $price_k$, $price^{electricity}$, $price^{steam}$, $price^{wd}$, $price^{heating}$, and $price^{cooling}$ are unit prices of related items or services; p^{om} is the percentage of the annualized investment cost into the O&M cost; K^{WT} is the subset of liquid species; $time_{l,i,j}$ denotes the specific annual operating time of technology j in section i and location l. I^{Wt} is the subset of waste treatment sections.

$$Aoc_l = \sum_{t \in T, k \in K} Fsc_{t,l,k} + \sum_{t \in T} (Wtc_{t,l} + Uc_{t,l}) + Omc_l, \quad \forall\, l \in L \tag{A.26}$$

$$Fsc_{t,l,k} = \sum_{i \in I, j \in J} price_k \cdot time_{t,i,j} \cdot Mr_{t,l,i,j,k}^{makeup}, \quad \forall\, t \in T,\ l \in L,\ k \in K \tag{A.27}$$

$$Uc_{t,l} = hour_t \cdot [price^{electricity} \cdot Npcr_{t,l} + price^{heating} \cdot Nhcr_{t,l} + price^{cooling} \cdot Nccr_{t,l}], \quad \forall\, t \in T,\ l \in L \tag{A.28}$$

$$Omc_l = p^{om} \cdot Aic_l, \quad \forall\, l \in L \tag{A.29}$$

$$Wtc_{t,l} = price^{wd} \cdot \sum_{i \in I^{WT}, j \in J, k \in K^{WT}} time_{t,i,j} \cdot Mr_{t,l,i,j,k}^{emission}, \quad \forall\, t \in T,\ l \in L \tag{A.30}$$

If we consider the revenue from selling glycerol, fertilizer, and surplus electricity and heating utility as a credit of biofuel production, the revenue, calculated by eq A.31 offsets part of the annualized cost. The net cost is then defined by eq A.32.

$$Cr_{t,l} = hour_t \cdot \left\{ \frac{price^{glycerol}}{\rho^{glycerol}} \cdot \sum_{i \in I, j \in J} Mr_{t,l,i,j,glycerol}^{down} + price^{fer} \cdot \sum_{i \in I, j \in J} Mr_{t,l,i,j,solid}^{down} + price^{electricity} \cdot Nppr_{t,l} \right\}, \quad \forall\, t \in T,\ l \in L \tag{A.31}$$

$$Nc_l = Aic_l + Aoc_l - \sum_{t \in T} Cr_{t,l} \tag{A.32}$$

Life Cycle Environmental Impact Analysis Constraints

The annual quantities of species k to quantify the life cycle environmental impact in the raw materials acquisition stage are defined by eq A.33. Their contributions to the GHG emissions add up to Gwp^{rma} in eq A.34, where the φ_k^{rma} values are the damage factors of the corresponding entries specified by the publications of the Intergovernmental Panel on Climate Change.

$$Lci_{t,l,k}^{rma} = \sum_{i \in I, j \in J} time_{t,i,j} \cdot Mr_{t,l,i,j,k}^{makeup}, \quad \forall\, t \in T,\ l \in L,\ k \in K \tag{A.33}$$

$$Gwp_l^{rma} = \sum_{t \in T, k \in K} \phi_k^{rma} \cdot Lci_{t,l,k}^{rma} \tag{A.34}$$

Following a similar manner, the contributions to the GHG emissions associated with the transportation and manufacturing stages are defined by eqs A.35–A.39.

$$Lci_{t,l}^{tran,fer} = Lci_{t,l,solid}^{rma} \cdot d^{fer}, \quad \forall\, t \in T,\ l \in L \tag{A.35}$$

$$Lci_{t,l}^{tran,chem} = \sum_{k \in K^{chem}} Lci_{t,l,k}^{rma} \cdot d^{chem}, \quad \forall\, t \in T,\ l \in L \tag{A.36}$$

$$Gwp_l^{tran} = \sum_{t \in T} \phi^{tran,truck} \cdot (Lci_{t,l}^{tran,fer} + Lci_{t,l}^{tran,chem}), \quad \forall\, l \in L \tag{A.37}$$

$$Lci_{t,l,k}^{de} = \sum_{i \in I, j \in J} time_{t,i,j} \cdot Mr_{t,l,i,j,k}^{emission} + (hour_t - time_{t,cultivation,openpond}) \sum_{i \in I, j \in J} Mr_{t,l,i,j,k}^{recycle}, \quad \forall\, t \in T,\ l \in L,\ k \in K \tag{A.38}$$

DOI: 10.1021/sc5008253
ACS Sustainable Chem. Eng. 2015, 3, 841–861

$$Gwp_l^{man} = \sum_{t\in T} [\phi_k^{de}\cdot Lci_{t,l,k}^{de} + hour_t\cdot (\phi^{ele}\cdot Npcr_{t,l} + \phi^{heat}\cdot Nhcr_{t,l} + \phi^{cool}\cdot Nccr_{t,l})], \quad \forall\, l \in L \tag{A.39}$$

$$Gwp_l^{CR} = \sum_{t\in T, j\in J} \phi_{glycerol}\cdot hour_t\cdot Mr_{t,l,upgrading,j,glycerol}^{down} + \sum_{t\in T, l\in L, j\in J} \phi_{fertilizer}\cdot hour_t \cdot (Mr_{t,l,upgrading,j,fertilizer}^{down} + Mr_{t,l,ad,j,fertilizer}^{down}) + \sum_{t\in T, l\in L, j\in J} \phi^{ele}\cdot hour_t\cdot Nppr_{t,l}, \quad \forall\, l \in L \tag{A.40}$$

Finally, the total environmental impact is determined as the sum of the above contributions.

$$Gwp_l = Gwp_l^{rma} + Gwp_l^{tran} + Gwp_l^{man} - Gwp_l^{CR} \tag{A.41}$$

APPENDIX B: INPUT DATA OF THE CASE STUDY

Table B1. Information for Facilities in CCUS Supply Chain

Power plants[82,86]

Location	Longitude	Latitude	CO_2 emissions (Mt/year)	CO_2 capture cost ($/t)
Monticello	−95.04	33.09	6.59	31.75
Martin Lake − Pirkey	−94.57	32.26	11.86	33.79
Sandow No. 4	−97.06	30.56	4.53	34.47
Coleto Creek	−97.21	28.71	5.66	37.64
WA Parish	−95.64	29.48	4.74	28.33

Geological sink[11,86]

Location	Longitude	Latitude	Storage capacity (Mt/year)	Sequestration cost ($/t)
Midland	−102.10	32.00	1,521.60	12

Algal biorefineries[48]

Location	Longitude	Latitude	Land availability (ha)
Red River − Bowie	−94.98	33.61	64,000
Panola	−94.32	32.19	20,000
Milam	−96.98	30.81	15,000
Wharton	−96.15	29.37	25,000
Goliad	−97.35	28.57	15,000

Biofuel terminals[87,88]

Location	Longitude	Latitude	Demand for biodiesel?	Demand for renewable diesel?
Dallas	−96.71	32.85	Yes	Yes
Waskom	−94.06	32.48	Yes	Yes
Mt. Pleasant	−94.97	33.16	No	Yes
Austin	−97.75	30.25	Yes	Yes
Houston	−95.42	29.80	Yes	Yes
Victoria	−97.00	28.81	No	Yes
Waco	−97.15	31.55	No	Yes

Table B2. CO_2 Mass Flow Rate Limits in Pipelines

Supercritical CO_2 pipelines[22,89]

Symbol	Nominal diameter (inches)	Flow rate lower bound (Mt CO_2/year)	Flow rate upper bound (Mt CO_2/year)
d4	4	0	0.190
d6	6	0.152	0.540
d8	8	0.432	1.130
d12	12	0.904	3.250
d16	16	2.600	6.860
d20	20	5.488	12.260
d24	24	9.808	19.690
d30	30	15.752	35.160
d36	36	28.128	56.460

Feed gas pipelines[90,91]

Symbol	Nominal diameter (inches)	Flow rate lower bound (Mt feed gas/year)	Flow rate upper bound (Mt feed gas/year)
dg48	48	8.976	15.456
dg58	58	12.360	24.300
dg72	72	19.440	40.200
dg84	84	32.160	56.520
dg96	96	45.216	77.208
dg108	108	61.764	100.320

Nomenclature

Notations for the supply chain model and the process model are given in this section. Units of the parameters and variables are given in brackets.

Notations for Supply Chain Model

Sets

- *dia* set of pipeline diameters for supercritical CO_2 transportation
- *diag* set of pipeline diameters for feed gas transportation
- *l* set of locations
- *mds* set of operating modes
- *prd* set of biofuel products
- *t* set of time periods

Subsets

- Adj_l subset of adjacent locations to *l* to which supercritical CO_2 can be transported
- *Bio* subset of algal biorefineries
- *Lcus* subset of biofuel terminals
- Nbr_l subset of nearby locations to *l* to which feed gas can be transported
- *Pow* subset of power plants
- *Sink* subset of geological sinks

Parameters

- $acd_{l,t}$ CO_2 emissions available at power plant *l* in time period *t* (t CO_2/month)
- c_l^{cap} unit cost for CO_2 capture at power plant *l* ($/t CO_2)
- cg_l^{cap} unit cost for retrieving feed gas at power plant *l* ($/t CO_2)
- $c_{l,lp,prd}^{dist}$ unit cost for shipping biofuel *prd* from location *l* to *lp* ($/gallon)
- $c_{l,lp,dia}^{pipe}$ capital cost for installing supercritical CO_2 pipeline with diameter *dia* from location *l* to *lp* ($)
- $cg_{l,lp,diag}^{pipe}$ capital cost for installing feed gas pipeline with diameter *diag* from location *l* to *lp* ($)

DOI: 10.1021/sc5008253
ACS Sustainable Chem. Eng. 2015, 3, 841−861

$c_{l,t}^{sink}$ unit cost for injection of supercritical CO_2 at geological sink l in time period t ($/t CO_2)
$dis_{l,lp}$ pipeline distance from location l to lp (km)
$dm_{l,prd,t}^{U}$ demand upper bound for biofuel prd at biofuel terminal l in time period t (gallon/month)
$dm_{l,prd,t}^{L}$ demand lower bound for biofuel prd at biofuel terminal l in time period t (gallon/month)
e_l^{cap} unit GHG emissions from CO_2 capture processes (t CO_2-equivalent/t CO_2)
eg_l^{cap} unit GHG emissions from feed gas retrieving (t CO_2-equivalent/t CO_2)
$e_{prd}^{displace}$ GHG emissions credit for producing unit biofuel prd (t CO_2-equivalent/gallon)
$e_{l,lp,prd}^{dist}$ unit GHG emissions from shipping biofuel prd from location l to lp (t CO_2-equivalent/gallon)
$e_{l,t}^{inj}$ unit GHG emissions from supercritical CO_2 injection (t CO_2-equivalent/t CO_2)
$e_{l,lp}^{pipe}$ unit GHG emissions from operations of the supercritical CO_2 pipeline from location l to lp (t CO_2-equivalent/t CO_2/km)
$eg_{l,lp}^{pipe}$ unit GHG emissions from operations of the feed gas pipeline from location l to lp (t CO_2-equivalent/t CO_2/km)
$ftrn_{l,lp,prd,t}^{U}$ transportation capacity of biofuel prd from algal biorefinery l to biofuel terminal lp in time period t (gallon/month)
ir discount rate (%)
$land_l$ land area available at algal biorefinery candidate site l (ha)
ls project lifetime (year)
$price_{l,prd,t}$ market price of biofuel prd at biofuel terminal l in time period t ($/gallon)
$inct_{prd}$ volumetric incentive for biofuel prd ($/gallon)
$qm_{l,lp}$ CO_2 flow rate upper bound between location l and lp (t CO_2/month)
q_{dia}^{U} maximum allowable flow rate in supercritical CO_2 pipeline with diameter dia (t supercritical CO_2/month)
q_{dia}^{L} minimum allowable flow rate in supercritical CO_2 pipeline with diameter dia (t supercritical CO_2/month)
qg_{diag}^{U} maximum allowable flow rate in feed gas pipeline with diameter dia (t feed gas/month)
qg_{diag}^{L} minimum allowable flow rate in feed gas pipeline with diameter dia (t feed gas/month)
$scap_l$ maximum injection rate of geological sink l (t CO_2/month)
tgt_l CO_2 emissions reduction target at power plant l (%)
$v_{l,lp,dia}^{pipe}$ O&M cost per unit length of supercritical CO_2 pipeline ($/km)
$vg_{l,lp,diag}^{pipe}$ O&M cost per unit length of feed gas pipeline ($/km)
wf weight factor to calculate the feed gas flow rate (%)
$\eta_{l,t}$ loss factor of CO_2 emissions at power plant l in time period t (%)
$\tau_{t,mds}$ length of operating mode mds in time period t (%)

Binary Variables

Xb_l One if algal biorefinery is built at location l; 0 otherwise
$Xp_{l,lp,t,mds}$ One if there is positive flow of supercritical CO_2 from location l to lp in time period t in operating mode mds; 0 otherwise
$Xpg_{l,lp,t,mds}$ One if there is positive flow of feed gas from location l to lp in time period t in operating mode mds; 0 otherwise
$Yp_{l,lp,dia}$ One if pipeline with diameter dia is built from location l to lp for transport of supercritical CO_2; 0 otherwise
$Ypg_{l,lp,diag}$ One if pipeline with diameter $diag$ is built from location l to lp for transport of feed gas; 0 otherwise

Continuous Variables

C^{bio} annualized cost of algal biorefineries, including capital and O&M cost ($/year)
$C^{capture}$ on-site carbon capture cost ($/year)
$C^{distribution}$ biofuel distribution cost ($/year)
$C^{pipe\_capical}$ capital cost for installing pipelines ($/year)
C^{pipe_om} pipeline O&M cost ($/year)
$C^{revenue}$ revenue from biofuel sales ($/year)
$C^{sequestration}$ CO_2 sequestration cost ($/year)
E^{bio} GHG emissions from algal biorefinery operations (t CO_2-equivalent/year)
$E^{capture}$ GHG emissions from CO_2 capture and retrieving processes (t CO_2-equivalent/year)
E^{credit} GHG emissions credit from production of renewable biofuels (t CO_2-equivalent/year)
$E^{distribution}$ GHG emissions from biofuel distribution (t CO_2-equivalent/year)
$E^{injection}$ GHG emissions from CO_2 injection processes (t CO_2-equivalent/year)
E^{pipe} GHG emissions from pipeline operations (t CO_2-equivalent/year)
$Ftrn_{l,lp,prd,t}$ amount of biofuel prd shipped from location l to lp in time period t (gallon/month)
$Gcd_{l,t,mds}$ amount of CO_2 captured at power plant l in time period t in operating mode mds (t CO_2/month)
$Ggcd_{l,t,mds}$ amount of CO_2 retrieved as feed gas at power plant l in time period t in operating mode mds (t CO_2/month)
$Hcd_{l,t,mds}$ amount of CO_2 utilized at algal biorefinery l in time period t in operating mode mds (t CO_2/month)
$Qcd_{l,lp,t,mds}$ amount of supercritical CO_2 transported from location l to lp in time period t in operating mode mds (t CO_2/month)
$Qgcd_{l,lp,t,mds}$ amount of CO_2 in feed gas transported from location l to lp in time period t in operating mode mds (t CO_2/month)
$Sales_{l,prd,t}$ sales amount of biofuel prd sold at biofuel terminal l in time period t (gallon/month)
$Scd_{l,t}$ amount of CO_2 injected at geological sink l in time period t (t CO_2/month)
$Wprd_{l,prd,t}$ amount of biofuel prd produced at algal biorefinery l in time period t (gallon/month)
$Zp_{l,lp,dia,t,mds}$ one if supercritical CO_2 pipeline with diameter dia from location l to lp is in use in time period t in operating mode mds; 0 otherwise
$Zpg_{l,lp,diag,t,mds}$ one if feed gas pipeline with diameter $diag$ from location l to lp is in use in time period t in operating mode mds; 0 otherwise

Notations for Process Model

Sets/Indices

I set of sections indexed by i
J set of technological alternatives indexed by j

DOI: 10.1021/sc5008253
ACS Sustainable Chem. Eng. 2015, 3, 841−861

K set of species indexed by k. The 37 species represent respectively H_2O, CO_2, N_2, O_2, H_2, CO, CH_4, C_2H_6, C_3H_8, C_4H_{10}, C_5H_{12}, polyelectrolyte, sodium hydroxide (flocculant), polyaluminum chloride, aluminum sulfate, chitosan, poly-γ-glutamic acid, N, P, algae, salt, lipid, remnant, hexane, isopropanol/hexane, butanol, solid, CH_4O, NaOH (catalyst), H_2SO_4, lipase, CH_3NaO, heterogeneous catalyst, glycerol, soap, biodiesel, and renewable diesel

N set of name of flows n represent respectively "up", "down", "in", "out", "makeup", "reuse", "recycle", "emission"

Subsets

C_i subset of species that contribute to $m_{i,j}^{cc}$ in section i

D_i subset of sections whose "down" flows go to section i

G subset of species that are the major components in natural gas

I^{wt} subset of waste treatment sections

K^{chem} subset of species for chemicals used in life cycle analysis

K^{WT} subset of liquid species

R_i subset of sections whose "recycle" flows go to section i

Parameters

$cc_{i,j}^{b}$ capital cost of technology j in section i in the base case ($)

$cepci_{i,j}$ chemical engineering plant cost index of the reference year

$cepci_{i,j}^{b}$ chemical engineering plant cost index of the base year

d^{fer} transportation distance for fertilizers (km)

d^{chem} transportation distance for chemicals (km)

$hour_t$ length of time period t (h)

ir discount rate

lhv_k lower heating value of species k (mWh/t)

ls life span of the project (year)

$m_{i,j}^{b}$ mass flow rate of technology j in section i in the base case (t/h)

$p_{i,j,k,k'}^{in}$ concentration of species k based on species k' in the "in" flow of technology j in section i

p^K total investment cost multiplier on based on the total capital cost

$price_k$ unit price of species k ($/t)

$price^{cooling}$ unit cooling cost ($/mWh)

$price^{electricity}$ unit electricity cost ($/mWh)

$price^{heating}$ unit heating cost ($/mWh)

$price^{land}$ unit land cost ($/ha)

$price^{steam}$ unit steam cost ($/mWh)

$price^{wd}$ unit waste disposal cost ($/t)

pro area productivity of the open pond in the cultivation section (t/h/ha)

$sc_{i,j,k,k'}$ stoichiometric coefficient of species k based on species k' in the reaction of technology j in section i

$sf_{i,j,k,k'}^{down}$ split fraction of species k of technology j in section i to the "down" flow on the basis of species k'

$sf_{i,j,k}^{emission}$ split fraction of species k of technology j in section i into the "emission" flow

$time_{t,i,j}$ length of operating times of technology j in section i in time period t (h)

ub upper bound of mass flow rate (t/h)

$ucc_{i,j,k}$ unit cooling consumption of species k of technology j in section i (mWh/t)

$uhc_{i,j,k}$ unit heat consumption of species k of technology j in section i (mWh/t)

$upc_{i,j,k}$ unit power consumption of species k of technology j in section i (mWh/t)

wf_k^{CO2} weight fraction of feed gas

$x_{t,i,j}$ reaction conversion of technology j in section i in time period t

$\eta^{turbine}$ energy conversion efficiency of the turbine

$\rho^{glycerol}$ density of glycerol (kg/m^3)

φ^{cool} impact factor of cooling (kg CO_2-equivalent/kWh)

φ_k^{de} impact factor of direct emissions of species k (kg CO_2-equivalent/kg)

φ^{ele} impact factor of electricity (kg CO_2-equivalent/kWh)

φ^{heat} impact factor of heating (kg CO_2-equivalent/kWh)

$\varphi^{tran,truck}$ impact factor of truck transportation (kg CO_2-equivalent/km/t)

Binary Variables

$Y_{l,i,j}$ one if technology j in section i is selected in algal biorefinery l; 0 otherwise

Continuous Variables

Aic_l annual investment cost of algal biorefinery l ($/year)

Aoc_l annual operation cost at algal biorefinery l ($/year)

$Area_l$ land area occupied by the open pond cultivation facilities (ha)

$Cc_{l,i,j}$ capital cost of technology j in section i at algal biorefinery l ($)

$Ccr_{t,l,i}$ cooling consumption rate in section i at algal biorefinery l in time period t (mW)

$Cr_{t,l}$ credit of algal biorefinery l in time period t ($/year)

$Fsc_{t,l,k}$ feedstock cost of species k at algal biorefinery l in time period t ($/t)

Gwp_l total global warming potential at algal biorefinery l (t CO_2-equivalent/year)

Gwp_l^{CR} global warming potential credit at algal biorefinery l (t CO_2-equivalent/year)

Gwp_l^{man} global warming potential of manufacturing at algal biorefinery l (t CO_2-equivalent/year)

Gwp_l^{rma} global warming potential of raw materials at algal biorefinery l (t CO_2-equivalent/year)

Gwp_l^{tran} global warming potential of transportation of algal biorefinery l (t CO_2-equivalent/year)

$Hcr_{t,l,i}$ heat consumption rate of section i at algal biorefinery l in time period t (mW)

$Hcd_{l,t}^{hr}$ total mass flow of the feed gas at algal biorefinery l in time period t (t/h)

Lc_l land cost at algal biorefinery l ($)

$Lci_{t,l,k}^{de}$ mass of species k at algal refinery l in time period t in direct emissions (t)

$Lci_{t,l,k}^{rma}$ mass of species k at algal refinery l in time period t for raw materials (t)

$Lci^{tran,fer}$ mass of species k at algal refinery l in time period t for transportation of fertilizers (t)

$Lci_{t,l}^{tran,chem}$ mass of species k at algal refinery l in time period t for transportation of chemicals (t)

$M_{l,i,j}$ auxiliary mass flow rate variable of technology j in section i at algal biorefinery l (t/h)

$Mc_{l,i,j,k}^{n}$ capacity of species k in flow n of technology j of section i in algal biorefinery l (t)

$Mr_{t,l,i,j,k}^{n}$ mass flow rate of species k in flow n of technology j of section i in algal biorefinery l in time period t (t/h)

$Nccr_{t,l}$ net cooling consumption rate at algal biorefinery l in time period t (mW)

$Nhcr_{t,l}$ net heat consumption rate at algal biorefinery l in time period t (mW)

DOI: 10.1021/sc5008253
ACS Sustainable Chem. Eng. 2015, 3, 841−861

$Npcr_{t,l}$ net power consumption rate of section i at algal biorefinery l (mW)
$Nppr_{t,l}$ net power production rate al algal biorefinery l in time period t (mW)
Omc_l O&M cost at algal biorefinery l ($/year)
$Pcr_{t,l,i}$ power consumption rate of section i at algal biorefinery l in time period t (mW)
$Ptr_{t,l}$ amount of electricity offset by the electricity supplies (mWh)
$Tpic_l$ total investment cost for algal biorefinery l ($)
$Uc_{t,l}$ utility cost of algal biorefinery l in time period t ($/mWh)
$Wtc_{t,l}$ waste disposal cost at algal biorefinery l in time period t ($/t)

AUTHOR INFORMATION

Corresponding Author

*Tel: +1 847 467 2943. Fax: +1 847 491 3728. E-mail: you@northwestern.edu.

Notes

The authors declare no competing financial interest.

ACKNOWLEDGMENTS

We gratefully acknowledge the financial support from the Institute for Sustainability and Energy at Northwestern University (ISEN).

REFERENCES

(1) Haszeldine, R. S. Carbon capture and storage: How green can black be? *Science* **2009**, *325*, 1647−1652.
(2) Lackner, K. S. A Guide to CO_2 Sequestration. *Science* **2003**, *300*, 1677−1678.
(3) National Research Council. *Advancing the Science of Climate Change*; The National Acdemies Press: Washington, DC, 2010.
(4) Center for Climate and Energy Solutions. *EPA Regulations of Greenhouse Gas Emissions from New Power Plants*, 2013. http://www.c2es.org/federal/executive/epa/ghg-standards-for-new-power-plants (accessed 2015).
(5) U.S. Environmental Protection Agency. *History of the Clean Air Act*. http://www.epa.gov/air/caa/amendments.html (accessed 2014).
(6) U.S. Environmental Protection Agency *Regulatory Impact Analysis for the Proposed Carbon Pollution Guidelines for Existing Power Plants and Emission Standards for Modified and Reconstructed Power Plants*, 2014. http://www2.epa.gov/sites/production/files/2014-06/documents/20140602ria-clean-power-plan.pdf (accessed 2015).
(7) White, C. M.; Strazisar, B. R.; Granite, E. J.; Hoffman, J. S.; Pennline, H. W. Separation and capture of CO_2 from large stationary sources and sequestration in geological formations—Coalbeds and deep saline aquifers. *J. Air Waste Manage. Assoc.* **2003**, *53*, 645−715.
(8) Rackley, S. *Carbon Capture and Storage*; Gulf Professional Publishing: Houston, TX2009.
(9) Wilcox, J. *Carbon Capture*; Springer: New York, 2012.
(10) Folger, P. *Carbon Capture and Sequestration: Research, Development, and Demonstration at the U.S. Department of Energy*; Congressional Research Service, 2014. https://www.fas.org/sgp/crs/misc/R42496.pdf (accessed 2015).
(11) Metz, B.; Davidson, O.; De Coninck, H.; Loos, M.; Meyer, L. *Carbon Dioxide Capture and Storage*; IPPC Special Report; Cambridge University Press: Cambridge, U.K., 2005.
(12) Szulczewski, M. L.; MacMinn, C. W.; Herzog, H. J.; Juanes, R. Lifetime of carbon capture and storage as a climate-change mitigation technology. *Proc. Natl. Acad. Sci. U. S. A.* **2012**, *109*, 5185−5189.
(13) Boot-Handford, M. E.; Abanades, J. C.; Anthony, E. J.; Blunt, M. J.; Brandani, S.; Mac Dowell, N.; Fernandez, J. R.; Ferrari, M.-C.; Gross, R.; Hallett, J. P.; Haszeldine, R. S.; Heptonstall, P.; Lyngfelt, A.; Makuch, Z.; Mangano, E.; Porter, R. T. J.; Pourkashanian, M.; Rochelle, G. T.; Shah, N.; Yao, J. G.; Fennell, P. S. Carbon capture and storage update. *Energy Environ. Sci.* **2014**, *7*, 130−189.
(14) Pedroni, P.; Davison, J.; Beckert, H.; Bergman, P.; Benemann, J. *A Proposal to Establish an International Network on Biofixation of CO_2 and Greenhouse Gas Abatement with Microalgae*; Proceedings of the U.S. Department of Energy/NETL 1st National Conference on Carbon Sequestration, May 2001.
(15) Yue, D.; You, F.; Snyder, S. W. Biomass-to-bioenergy and biofuel supply chain optimization: Overview, key issues and challenges. *Comput. Chem. Eng.* **2014**, *66*, 36−56.
(16) Benemann, J. R.; Pedroni, P. Biofixation of fossil CO_2 by microalgae for greenhouse gas abatement. In *Encyclopaedia of Hydrocarbons*; Treccani, P., Ed.; **2008**; Vol. *III*, New Developments: Energy, Transport, Sustainability, Chapter 9.
(17) Moody, J. W.; McGinty, C. M.; Quinn, J. C. Global evaluation of biofuel potential from microalgae. *Proc. Natl. Acad. Sci. U. S. A.* **2014**, *111*, 8691−8696.
(18) Dooley, J. J.; Dahowski, R.; Davidson, C.; Wise, M.; Gupta, N.; Kim, S.; Malone, E. Carbon Dioxide Capture and Geologic Storage. In *Second Phase of the Global Energy Technology Strategy Program*, 2006.
(19) Rostam-Abadi, M.; Chen, S. S.; Lu, Y. *Assess Carbon Dioxide Capture Options for Illinois Basin Carbon Dioxide Sources*; Illinois State Geological Survey: Champaign, IL, 2005.
(20) Kazmierczak, T.; Brandsma, R.; Neele, F.; Hendriks, C. Algorithm to create a CCS low-cost pipeline network. *Energy Procedia* **2009**, *1*, 1617−1623.
(21) Middleton, R. S.; Bielicki, J. M. A scalable infrastructure model for carbon capture and storage: SimCCS. *Energy Policy* **2009**, *37*, 1052−1060.
(22) Middleton, R. S.; Kuby, M. J.; Bielicki, J. M. Generating candidate networks for optimization: The CO_2 capture and storage optimization problem. *Comput., Environ., Urban Syst.* **2012**, *36*, 18−29.
(23) Morbee, J.; Serpa, J.; Tzimas, E. Optimised deployment of a European CO_2 transport network. *Int. J. Greenhouse Gas Control* **2012**, *7*, 48−61.
(24) Middleton, R. S.; Brandt, A. R. Using infrastructure optimization to reduce greenhouse gas emissions from oil sands extraction and processing. *Environ. Sci. Technol.* **2013**, *47*, 1735−1744.
(25) Zhou, C.; Liu, P.; Li, Z. A superstructure-based mixed-integer programming approach to optimal design of pipeline network for large-scale CO_2 transport. *AIChE J.* **2014**, *60*, 2442−2461.
(26) Gutiérrez-Arriaga, C. G.; Serna-González, M.; Ponce-Ortega, J. M.; El-Halwagi, M. M. Sustainable integration of algal biodiesel production with steam electric power plants for greenhouse gas mitigation. *ACS Sustainable Chem. Eng.* **2014**, *2*, 1388−1403.
(27) Silva, C.; Soliman, E.; Cameron, G.; Fabiano, L. A.; Seider, W. D.; Dunlop, E. H.; Coaldrake, A. K. Commercial-scale biodiesel production from algae. *Ind. Eng. Chem. Res.* **2013**, *53*, 5311−5324.
(28) Pokoo-Aikins, G.; Nadim, A.; El-Halwagi, M.; Mahalec, V. Design and analysis of biodiesel production from algae grown through carbon sequestration. *Clean Technol. Environ. Policy* **2010**, *12*, 239−254.
(29) Gong, J.; You, F. Optimal design and synthesis of algal biorefinery processes for biological carbon sequestration and utilization with zero direct greenhouse gas emissions: MINLP model and global optimization algorithm. *Ind. Eng. Chem. Res.* **2014**, *53*, 1563−1579.
(30) Gebreslassie, B. H.; Waymire, R.; You, F. Sustainable design and synthesis of algae-based biorefinery for simultaneous hydrocarbon biofuel production and carbon sequestration. *AIChE J.* **2013**, *59*, 1599−1621.
(31) Kadam, K. L. *Microalgae Production from Power Plant Flue Gas: Environmental Implications on a Life Cycle Basis*; NREL/TP-510-29417; National Renewable Energy Laboratory, 2001.
(32) *National Algal Biofuels Technology Roadmap*; U.S. Department of Energy, Office of Energy Efficiency and Renewable Energy, Biomass Program, 2010.

DOI: 10.1021/sc5008253
ACS Sustainable Chem. Eng. 2015, 3, 841−861

(33) Colliver, A. *Low-Emission Technology Series: Introduction to Carbon Capture and Storage*; Commonwealth Scientific and Industrial Research Organisation (CSIRO) and the Global CCS Institute, 2012.
(34) Hester, R. E.; Harrison, R. M.; Chemistry, R. S. o. *Carbon Capture: Sequestration and Storage*; Royal Society of Chemistry, 2010.
(35) Smit, B.; Reimer, J. R.; Oldenburg, C. M.; Bourg, I. C. *Introduction to Carbon Capture and Sequestration*; World Scientific, 2014.
(36) Metz, B.; Davidson, O.; De Coninck, H.; Loos, M.; Meyer, L. *IPCC Special Report on Carbon Dioxide Capture and Storage*. Working Group III of the Intergovernmental Panel on Climate Change; Cambridge University Press: Cambridge, U.K, 2005; Volume *4*.
(37) MacDowell, N.; Florin, N.; Buchard, A.; Hallett, J.; Galindo, A.; Jackson, G.; Adjiman, C. S.; Williams, C. K.; Shah, N.; Fennell, P. An overview of CO_2 capture technologies. *Energy Environ. Sci.* **2010**, *3*, 1645−1669.
(38) Rubin, E. S. CO_2 capture and transport. *Elements* **2008**, *4*, 311−317.
(39) Dooley, J.; Dahowski, R.; Davidson, C.; Wise, M.; Gupta, N.; Kim, S.; Malone, E. *Carbon Dioxide Capture and Geologic Storage*; Global Energy Technology Strategy Program, 2006.
(40) CO_2 Pipeline Infrastructure, 2013. IEAGHG. http://ieaghg.org/publications/blog/118-general/441-ieaghg-report-on-co2-pipeline-infrastructure (accessed 2015).2013.
(41) CO_2 Sources, Denbury. http://www.denbury.com/operations/gulf-coast-region/co2-sources-and-pipelines/default.aspx (accessed March 3, 2015).
(42) Blunt, M.; Fayers, F. J.; Orr, F. M., Jr. Carbon dioxide in enhanced oil recovery. *Energy Convers. Manage.* **1993**, *34*, 1197−1204.
(43) Carbon Capture and Storage. Wikipedia. http://en.wikipedia.org/w/index.php?title=Carbon_capture_and_storage&oldid=633844952 (accessed November 21, 2014.
(44) MIT Carbon Capture and Sequestration Project Database. Massachusetts Institute of Technology. https://sequestration.mit.edu/tools/projects/ (accessed December 5, 2014).
(45) Review of the Feasibility of Carbon Dioxide Capture and Storage in the UK. DTI. http://www.cslforum.org/publications/documents/dti_review.pdf (accessed 2013).
(46) Hanagata, N.; Takeuchi, T.; Fukuju, Y.; Barnes, D. J.; Karube, I. Tolerance of microalgae to high CO_2 and high temperature. *Phytochemistry* **1992**, *31*, 3345−3348.
(47) Wigmosta, M. S.; Coleman, A. M.; Skaggs, R. J.; Huesemann, M. H.; Lane, L. J. National microalgae biofuel production potential and resource demand. *Water Resour. Res.* **2011**, *47*, W00H04.
(48) Venteris, E. R.; Skaggs, R. L.; Coleman, A. M.; Wigmosta, M. S. A GIS cost model to assess the availability of freshwater, seawater, and saline groundwater for algal biofuel production in the United States. *Environ. Sci. Technol.* **2013**, *47*, 4840−4849.
(49) Venteris, E. R.; McBride, R. C.; Coleman, A. M.; Skaggs, R. L.; Wigmosta, M. S. Siting algae cultivation facilities for biofuel production in the United States: Trade-offs between growth rate, site constructability, water availability, and infrastructure. *Environ. Sci. Technol.* **2014**, *48*, 3559−3566.
(50) Gong, J.; You, F. Global optimization for sustainable design and synthesis of algae processing network for CO_2 mitigation and biofuel production using life cycle optimization. *AIChE J.* **2014**, *60*, 3195−3210.
(51) Farahipour, R.; Karunanithi, A. T. Life cycle environmental implications of CO_2 capture and sequestration with ionic liquid 1-butyl-3-methylimidazolium acetate. *ACS Sustainable Chem. Eng.* **2014**, *2*, 2495−2500.
(52) Bojarski, A. D.; Guillén-Gosálbez, G.; Jiménez, L.; Espuña, A.; Puigjaner, L. Life cycle assessment coupled with process simulation under uncertainty for reduced environmental impact: Application to phosphoric acid production. *Ind. Eng. Chem. Res.* **2008**, *47*, 8286−8300.
(53) Zhang, D.; Evangelisti, S.; Lettieri, P.; Papageorgiou, L. G. *Optimal Design of Microgrids with Innovative CHP Systems: Integration of Process Optimisation and Life Cycle Assessment*. In AIChE Annual Meeting, Atlanta, GA, 2014.
(54) Sengupta, D.; Mukherjee, R.; Sikdar, S. K. Environmental sustainability of countries using the UN MDG indicators by multivariate statistical methods. *Environ. Prog. Sustainable Energy* **2015**, *34*, 198−206.
(55) Gebreslassie, B. H.; Slivinsky, M.; Wang, B.; You, F. Life cycle optimization for sustainable design and operations of hydrocarbon biorefinery via fast pyrolysis, hydrotreating and hydrocracking. *Comput. Chem. Eng.* **2013**, *50*, 71−91.
(56) He, C.; You, F.; Feng, X. A novel hybrid feedstock to liquids and electricity process: Process modeling and exergoeconomic life cycle optimization. *AIChE J.* **2014**, *60*, 3739−3753.
(57) Garcia, D. J.; You, F. Multiobjective optimization of product and process networks: General modeling framework, efficient global optimization algorithm, and case studies on bioconversion. *AIChE J.* **2015**, *61*, 530−551.
(58) Wang, B.; Gebreslassie, B. H.; You, F. Sustainable design and synthesis of hydrocarbon biorefinery via gasification pathway: Integrated life cycle assessment and technoeconomic analysis with multiobjective superstructure optimization. *Comput. Chem. Eng.* **2013**, *52*, 55−76.
(59) *ISO 14040: Environmental Management-Life Cycle Assessment-Principles and Framework*; International Standard: ISO Standards, 2006.
(60) Bakshi, B. R. Methods and tools for sustainable process design. *Curr. Opin. Chem. Eng.* **2014**, *6*, 69−74.
(61) Cano-Ruiz, J. A.; McRae, G. J. Environmentally conscious chemical process design. *Annu. Rev. Energy Environ.* **1998**, *23*, 499−536.
(62) Hugo, A.; Pistikopoulos, E. Environmentally conscious long-range planning and design of supply chain networks. *J. Cleaner Prod.* **2005**, *13*, 1471−1491.
(63) You, F.; Tao, L.; Graziano, D. J.; Snyder, S. W. Optimal design of sustainable cellulosic biofuel supply chains: Multiobjective optimization coupled with life cycle assessment and input-output analysis. *AIChE J.* **2012**, *58*, 1157−1180.
(64) van Hermelen, T; Oonk, H. *Microalgae Biofixation Processes: Applications and Potential Contributions to Greenhouse Gas Mitigation Options*; EniTechnologie, 2006.
(65) IPCC Glossary. In *Fourth Assessment Report of the Intergovernmental Panel on Climate Change*, 2007.
(66) The Ecoinvent Database. Swiss Centre for Life Cycle Inventories, 2008. http://www.ecoinvent.ch/ (accessed 2015).
(67) Yue, D.; Kim, M. A.; You, F. Design of sustainable product systems and supply chains with life cycle optimization based on functional unit: General modeling framework, mixed-integer nonlinear programming algorithms and case study on hydrocarbon biofuels. *ACS Sustainable Chem. Eng.* **2013**, *1*, 1003−1014.
(68) Yue, D.; Slivinsky, M.; Sumpter, J.; You, F. Sustainable Design and Operation of Cellulosic Bioelectricity Supply Chain Networks with Life Cycle Economic, Environmental, and Social Optimization. *Ind. Eng. Chem. Res.* **2014**, *53*, 4008−4029.
(69) Sinnott, R. W. Virtues of the Haversine. *Sky Telescope* **1984**, *68*, 158.
(70) You, F.; Wang, B. Life cycle optimization of biomass-to-liquid supply chains with distributed−centralized processing networks. *Ind. Eng. Chem. Res.* **2011**, *50*, 10102−10127.
(71) Tawarmalani, M.; Sahinidis, N. V. A polyhedral branch-and-cut approach to global optimization. *Math. Program.* **2005**, *103*, 225−249.
(72) You, F.; Grossmann, I. E. Stochastic inventory management for tactical process planning under uncertainties: MINLP models and algorithms. *AIChE J.* **2011**, *57*, 1250−1277.
(73) You, F.; Pinto, J. M.; Grossmann, I. E.; Megan, L. Optimal distribution-inventory planning of industrial gases. II. MINLP models and algorithms for stochastic cases. *Ind. Eng. Chem. Res.* **2011**, *50*, 2928−2945.

DOI: 10.1021/sc5008253
ACS Sustainable Chem. Eng. 2015, 3, 841−861

(74) Yue, D.; You, F. Planning and scheduling of flexible process networks under uncertainty with stochastic inventory: MINLP models and algorithm. *AIChE J.* **2013**, *59*, 1511−1532.
(75) Yue, D.; You, F. Fair profit allocation in supply chain optimization with transfer price and revenue sharing: MINLP model and algorithm for cellulosic biofuel supply chains. *AIChE J.* **2014**, *60*, 3211−3229.
(76) Gong, J.; You, F. Value-added chemicals from microalgae: Greener, more economical, or both? *ACS Sustainable Chem. Eng.* **2015**, *3*, 82−96.
(77) Padberg, M. Approximating separable nonlinear functions via mixed zero-one programs. *Oper. Res. Lett.* **2000**, *27*, 1−5.
(78) Yue, D.; You, F. Game-theoretic modeling and optimization of multi-echelon supply chain design and operation under Stackelberg game and market equilibrium. *Comput. Chem. Eng.* **2014**, *71*, 347−361.
(79) Hasan, M.; Karimi, I. Piecewise linear relaxation of bilinear programs using bivariate partitioning. *AIChE J.* **2010**, *56*, 1880−1893.
(80) Gao, J.; You, F. Optimal design and operations of supply chain networks for water management in shale gas production: MILFP model and algorithms for the water-energy nexus. *AIChE J.* **2015**, *61*, 1184−1208.
(81) Bergamini, M. L.; Grossmann, I.; Scenna, N.; Aguirre, P. An improved piecewise outer-approximation algorithm for the global optimization of MINLP models involving concave and bilinear terms. *Comput. Chem. Eng.* **2008**, *32*, 477−493.
(82) Prasodjo, D.; Pratson, L. *OptimaCCS Carbon Capture and Storage Infrastructure Optimization: Texas Case Study*; Nicholas School of the Environment, Duke University, 2011.
(83) Texas Net Electricity Generation by Source, U.S. Energy Information Administration. http://www.eia.gov/state/?sid=TX (accessed December 3, 2014).
(84) Geisbrecht, R. A. *Retrofitting Coal-Fired Power Plants for Carbon Dioxide Capture and Sequestration: Exploratory Testing of NEMS for Integrated Assessments*; DOE/NETL-2008/1309; National Energy Technology Laboratory, 2008.
(85) GIS Data Nature Features Texas Terrain Color Ramp. Texas Water Development Board. https://www.twdb.state.tx.us/mapping/gisdata.asp (accessed December 4, 2014).
(86) Zhou, C.; Pratson, L. *Optimal Design of Pipelines Network for CO_2 Transport*; Duke University, 2014.
(87) Biodiesel Fueling Station Locations. U.S. Department of Energy. http://www.afdc.energy.gov/fuels/biodiesel_locations.html (accessed December 3, 2014).
(88) Texas State Profile and Energy Estimates. U.S. Energy Information Administration. http://www.eia.gov/state/?sid=TX#tabs- (accessed December 3, 2014).
(89) *Carbon Management GIS: CO_2 Pipeline Transport Cost Estimation*; Carbon Capture and Sequestration Technologies Program; Massachusetts Institute of Technology, 2009.
(90) About U.S. Natural Gas Pipelines. U.S. Energy Information Administration. http://www.eia.gov/pub/oil_gas/natural_gas/analysis_publications/ngpipeline/index.html (accessed December 3, 2014).
(91) Natural Gas Pipeline Sizing. CheCalc. http://checalc.com/solved/gasPipeSizing.html (accessed December 3, 2014).
(92) ZEP *CO_2 Capture and Storage (CCS): Recommendations for Transitional Measures to Drive Deployment in Europe*; Zero Emissions Platform, 2013.
(93) Electricity Data Browser. U.S. Energy Information Administration. http://www.eia.gov/electricity/data/browser/ (accessed December 3, 2014).
(94) Clean Cities Alternative Fuel Price Report. U.S. Department of Energy. http://www.afdc.energy.gov/uploads/publication/alternative_fuel_price_report_july_2014.pdf (accessed 2014).
(95) Yacobucci, B. D. *Biofuels Incentives: A Summary of Federal Programs*; Congressional Research Service, 2012.
(96) Sun or Moon Rise/Set Table for One Year. U.S. Naval Observatory. http://aa.usno.navy.mil/data/docs/RS_OneYear.php (accessed December 3, 2014).
(97) National Solar Radiation Data Base. National Renewable Energy Laboratory. http://rredc.nrel.gov/solar/old_data/nsrdb/ (accessed December 3, 2014).
(98) *Carbon Dioxide Transport and Storage Costs in NETL Studies*; DOE/NETL-2013/1614; National Energy Technology Laboratory, 2013.
(99) FE/NETL CO_2 Transport Cost Model. NETL. http://www.netl.doe.gov/research/energy-analysis/analytical-tools-and-data/co2-transport (accessed December 3, 2014).
(100) Khoo, H. H.; Tan, R. B. H. Life Cycle Investigation of CO_2 Recovery and Sequestration. *Environ. Sci. Technol.* **2006**, *40*, 4016−4024.
(101) Jaramillo, P.; Griffin, W. M.; McCoy, S. T. Life cycle inventory of CO_2 in an enhanced oil recovery system. *Environ. Sci. Technol.* **2009**, *43*, 8027−8032.
(102) McCoy, S. T. *The Economics of Carbon Dioxide Transport by Pipeline and Storage in Saline Aquifers and Oil Reservoirs*; ProQuest, 2008.
(103) GREET: The Greenhouse Gases, Regulated Emissions, and Energy Use in Transportation Model. Argonne National Laboratory. http://greet.es.anl.gov/ (accessed 2014).

DOI: 10.1021/sc5008253
ACS Sustainable Chem. Eng. 2015, 3, 841−861